The limits of evolutionary convergence in sympatry: reproductive interference and developmental constraints leading to local diversity in warning traits

Ludovic Maisonneuve[1,*]

Marianne Elias[1]

Charline Smadi[2]

Violaine Llaurens[1]

1. Institut de Systématique, Evolution, Biodiversité (ISYEB), Muséum national d'Histoire naturelle, CNRS, Sorbonne Université, EPHE, Université des Antilles CP 50, 57 rue Cuvier, 75005 Paris, France;

2. Univ. Grenoble Alpes, INRAE, LESSEM, F-38402 St-Martin-d'Hères, France and Univ. Grenoble Alpes, CNRS, Institut Fourier, 38610 Gières, France;

∗ Corresponding author; e-mail: ludovic.maisonneuve.2015@polytechnique.org.

Keywords: Mimicry, Reproductive interference, Convergence, Imperfect mimicry, Quantitative genetics.

Manuscript type: Article.

Abstract

Mutualistic interactions between defended species represent a striking case of evolutionary convergence in sympatry, driven by the increased protection against predators brought by mimicry in warning traits. However, such convergence is often limited: sympatric defended species frequently display different or imperfectly similar warning traits. The phylogenetic distance between sympatric species may indeed prevent evolution towards the exact same signal. Moreover, warning traits are also involved in mate recognition, so that trait convergence might result in heterospecific courtship and mating. Here, we develop a mathematical model to investigate the strength and direction of evolution of warning trait in defended species with different ancestral traits. Specifically, we determine the effect of phenotypic distances between ancestral trait states of sympatric defended species, and costs of heterospecific sexual interactions on imperfect mimicry and trait divergence. Our analytical results confirm that reproductive interference limits the convergence of warning traits, leading to either complete divergence, or imperfect mimicry, but only between species with different ancestral traits. Surprisingly, our model pinpoints that, depending on the relative species densities, the mimic/model relationships between sympatric species can be inverted. Our study suggests that reproductive interference may promote the emergence of novel warning traits, enhancing mimetic diversity.

Introduction

Evolutionary convergence of traits between species is often promoted by natural selection, but trait similarity between species may be impaired by contrasted developmental and ecological constraints encountered within the different converging species. Large phylogenetic distances between species, as well as strikingly different ancestral traits, may indeed affect the extent of convergence. Furthermore, when trait convergence occurs in sympatry, trait similarity may generate costs linked to reproductive interference, counter-selecting trait resemblance between species. Here we investigate the limits of evolutionary convergence in sympatry by focusing on the striking case of intra-guild mutualistic interactions.

Mutualistic interactions frequently drive convergent evolution of different traits in sympatric species, but the ecological factors determining the strength and direction of convergence are still largely unknown. For example, avian vocal resemblance has been suggested to allow the formation of mixed-species flocks that may benefit all individuals from the different species (Goodale and Kotagama, 2006); trait similarity between sympatric species may promote pollinator attraction in nectar-rewarding flowers (Benitez-Vieyra et al., 2007; Schemske, 1981). In aposematic species, where a warning trait advertises predators from defense, Müllerian mimicry, *i.e.* the convergence in warning trait among defended species is certainly the best documented case of mutualistic interactions driving trait evolution in sympatric species (Sherratt, 2008): the costs associated with predators' learning is indeed shared among all individuals displaying the same trait, regardless the species they belong to (*e.g.* in plants (Lev-Yadun, 2009), mollusks (Cortesi and Cheney, 2010), vertebrates (Sanders et al., 2006; Springer and Smith-Vaniz, 1972) and insects (Mallet and Gilbert Jr., 1995)). Field experiments report an intense selection exerted by predators favoring warning trait convergence in sympatry (Arias et al., 2016; Benson, 1972; Chouteau et al., 2016; Kapan, 2001; Mallet and Barton, 1989). Surprisingly, despite this intense selection, many sympatric defended species exhibit only imperfect resemblance (*e.g.* (Savage and Slowinski, 1992)) or even different warning traits (*e.g.* (Beccaloni, 1997)) (Briolat et al., 2019).

The level of trait convergence between sympatric species can vary because of other developmental or selective constraints that may differ among species. For example, diet (Grill and Moore, 1998; Ojala et al., 2007) has been shown to influence the warning trait, and can strongly differ among sympatric species, leading to different species-specific trade-offs limiting convergence. As highlighted by the significant phylogenetic signal observed on the warning trait of mimetic butterflies of the tribe Ithomiini (Chazot et al., 2014; Elias et al., 2008), developmental and historical constraints may strongly influence the evolution of warning traits. Theoretical studies suggest that ancestral trait states may play a key role in the evolution of warning traits because the convergence of trait can be facilitated by an initial resemblance between species (Balogh and Leimar, 2005; Franks and Noble, 2004; Franks and Sherratt, 2007). Other theoretical studies highlight that the level of standing genetic and phenotypic variance within species strongly influences convergence between species (Ruxton et al., 2008). The balance between (1) the shared predation pressure faced by individuals from different sympatric species and (2) the developmental or selective constraints within each species may thus strongly shape the evolutionary convergence in warning traits, and especially modify the direction of evolution of traits within the different defended species living in sympatry. While convergence (Sherratt, 2008) usually assumes a joint evolution of traits in several sympatric species toward resemblance (*e.g.* Flanagan et al. (2004); Symula et al. (2001)), resemblance might also emerged from advergence, whereby trait evolution occur in a given species (*i.e.* the 'mimic' species), leading to high similarity to the ancestral trait displayed in another species (*i.e.* the 'model' species) (see (Dalziell and Welbergen, 2016) for the terminology). The direction of advergence, whereby phenotypic evolution in the 'mimic' species preferentially heads towards the phenotype displayed in 'model' species could be inverted (*i.e.* with phenotypic evolution in the 'mimic' species promoting traits more dissimilar to those of the 'model' species), depending on the relative levels of defense between sympatric species.

Moreover, the convergence of warning traits in different species may entail costs due to behavioral interference, thereby limiting positive selection on trait resemblance. Warning traits are indeed frequently involved in species recognition (Jiggins et al., 2001; Kronforst et al., 2006; Mer-

rill et al., 2014; Naisbit et al., 2001), leading to risk of confusion during sexual interactions. Species sharing similar warning traits may thus be exposed to substantial reproductive interference incurring fitness costs during mate acquisition due to interspecific interactions, including heterospecific courtship and mating as well as heterospecific male rivalry (Gröning and Hochkirch, 2008). Such reproductive interference has been observed between species sharing similar warning traits (in *Heliconius* butterfly species for instance (Estrada and Jiggins, 2008)). However, empirical studies precisely estimating the level of reproductive interference in sympatric species are scarce. Pheromone differences between mimetic species have been documented to limit the rate of erroneous mating (see Darragh et al. (2017); González-Rojas et al. (2020) for empirical examples in *Heliconius* butterflies). However, the pheromones of day-flying butterflies usually act as short-distance cues that may be perceived only during the courtship (Mérot et al., 2015). Females deceived by the color pattern of the heterospecific males may have spent time and energy or may need to deploy substantial efforts to avoid heterospecific mating. Therefore, females may still suffer from cost associated to reproductive interference, even if females refuse mating with heterospecific males. When females are courted by heterospecific males displaying their preferred cue before being rejected, this results in increased costs associated with mate searching in males (*i.e.* signal jamming in (Gröning and Hochkirch, 2008)).

Reproductive interference can generate reproductive character displacement (Gröning and Hochkirch, 2008; Kyogoku, 2015), whereby reproductive traits are more dissimilar between species in sympatric than in allopatric populations (Brown and Wilson, 1956). Such reproductive character displacement may thus impair convergence driven by mutualistic interactions. Theoretical studies have investigated how the evolution of female preferences may promote reproductive character displacement in males (McPeek and Gavrilets, 2006; Yamaguchi and Iwasa, 2013): reproductive interference costs are predicted to favor the divergence of female preferences, therefore promoting the divergence of male reproductive traits through sexual selection. Nevertheless, numerical simulations show that the effect of reproductive interference on trait divergence is not straightforward, when those traits are under strong selection promoting convergence (Boussens-

Dumon and Llaurens, 2021). However, the outcomes of these antagonistic selective forces might range from trait divergence to full convergence, through limited convergence and cannot be investigated in models assuming only discrete and well-differentiated warning traits, calling for a theoretical framework providing general expectations on the gradual evolution of convergent traits.

Here, we thus investigate the ecological factors limiting the convergence of traits involved in mutualistic interactions, by building a mathematical model that describes the evolution of quantitative traits in a *focal* species involved in mutualistic interactions within a fixed community of defended species. We specifically study the evolution of (1) the quantitative trait t involved in mutualistic interaction, displayed in both males and females and (2) the preference p of females which value indicates male trait value preferred by the females. We assume that individuals gain protection against predators from the similarity of their warning trait t toward the trait displayed in the local community of defended species. However, trait similarity between species generates fitness costs for females *via* reproductive interference (McPeek and Gavrilets, 2006; Yamaguchi and Iwasa, 2013). We also investigate the effect of developmental and selective constraints by testing the effect of the ancestral trait value t_a on trait convergence. Using weak selection approximation (Barton and Turelli, 1991; Kirkpatrick et al., 2002), we obtain equations describing the evolution of the mean trait and mean preference values in the *focal* species. We then use analytical results and numerical analyses to investigate the effect of reproductive interference on the convergence of trait depending on different ecological factors. Finally, to specifically investigate the effect of reproductive interference and of ancestral trait values on the direction of advergence, we extend our model to two interacting species that exhibit different densities, individual levels of defense and ancestral trait values, and explore the joint evolution of displayed trait and female preference in both species.

Evolution of warning trait toward a fixed community of defended species

Methods

We consider a single species (refered to as *focal* species hereafter) living in sympatry with a community of defended species (referred to as the *local mimicry ring* hereafter). In the *local mimicry ring*, all individuals display a similar warning trait: we denote $\bar{t}'$ the mean value of the trait displayed in the *local mimicry ring*, assumed to be fixed. We then investigate the evolution of a trait within the *focal* species, influenced by both predators' behavior (promoting mimicry toward the local mimicry ring) and mate choice. This trait t is expressed in both males and females and we assume that only females express a mating preference for males with trait value close to the value of females' preference trait p. Individuals of the *focal* species benefit from increased survival when they display a trait similar to the *local mimicry ring* (mean trait value in the community, $\bar{t}'$) because of predators warning trait learning. This resemblance toward the *local mimicry ring* may induce costs for individuals from the *focal* species, because of reproductive interference. We thus assume increasing fitness costs due to RI, when the trait displayed by males from the *focal* species and trait displayed in the *local mimicry ring* become more similar (see Equation (12)).

We assume that the trait and preference in the *focal* species are quantitative traits, with an autosomal polygenic basis, and additive effects. We consider discrete and non-overlapping generations. Within each generation, both (1) natural selection acting on survival and (2) sexual selection acting on reproductive success do occur. Natural selection acting on an individual depends on the trait value t it expresses. We note $W_{ns}(t)$ (defined after in Equations (8)) the fitness components due to natural selection acting on an individual displaying the trait value t. To compute the fitness component due to reproduction, we then note $W_r(t_m, p_f)$ (defined after in Equation (7)) the contribution of a mating between a male with trait t_m and a female with

preference p_f to the next generation. We also compute $W_{RI}(p_f)$ (defined after in Equation (12) the female fitness component describing fitness reduction due to RI. Following (Kirkpatrick et al., 2002) the reproductive success $W(t_m, t_f, p_f)$ stemming from a mated pair of a male with trait t_m and a female with trait t_f and preference p_f is given by:

$$W(t_m, t_f, p_f) = W_{ns}(t_m) W_r(t_m, p_f) W_{ns}(t_f) W_{RI}(p_f). \tag{1}$$

Using the Price's theorem (see Rice (2004) for instance), we can approximate the change in the mean values of traits $\bar{t}_m, \bar{t}_f$ and preference $\bar{p}_f$ in the *focal* species after the natural and sexual selection respectively by:

$$\begin{pmatrix} \Delta \bar{t} \\ \Delta \bar{p} \end{pmatrix} = \frac{1}{2} \begin{pmatrix} G_t & C_{tp} \\ C_{tp} & G_p \end{pmatrix} \begin{pmatrix} \beta_t \\ \beta_p \end{pmatrix}, \tag{2}$$

where G_t and G_p are the genetic variances of the trait t and the preference p, and C_{tp} is the genetic covariance between t and p in the *focal* species. β_t and β_p describe the selective forces acting on the trait t and the preference p, respectively and are given by:

$$\beta_t := \frac{\partial}{\partial t_m} \ln W(t_m, t_f, p_f) + \frac{\partial}{\partial t_f} \ln W(t_m, t_f, p_f) \Big|_{(t_m, t_f, p_f) = (\bar{t}, \bar{t}, \bar{p})}, \tag{3}$$

$$\beta_p := \frac{\partial}{\partial p_f} \ln W(t_m, t_f, p_f) \Big|_{(t_m, t_f, p_f) = (\bar{t}, \bar{t}, \bar{p})}. \tag{4}$$

We assume weak natural and sexual selective pressures (Iwasa et al., 1991; Pomiankowski and Iwasa, 1993), *i.e.* that the difference of fitness between different individuals is at maximum of order ε, with ε being small. Under this hypothesis, genetic correlations generated by selection and non-random mating quickly reach equilibrium (Nagylaki, 1993) and can thus be approximated by their equilibrium values. Weak selection hypothesis also implies that the variance of traits and preference is low (Iwasa et al., 1991).

Following (Iwasa et al., 1991), we assume that G_t and G_p are positive constants maintained by an equilibrium between selection and recurrent mutations. Under weak selection, the genetic covariance between t and p can be approximated by (see Appendix 1.3):

$$C_{tp} = a G_t G_p. \tag{5}$$

Because under weak selection G_t and G_p are small, C_{tp} is small in comparison with G_t and G_p, allowing us to approximate the change in the mean values of trait and preference by:

$$\begin{pmatrix} \Delta\bar{t} \\ \Delta\bar{p} \end{pmatrix} \approx \frac{1}{2} \begin{pmatrix} G_t & 0 \\ 0 & G_p \end{pmatrix} \begin{pmatrix} \beta_t \\ \beta_p \end{pmatrix} = \frac{1}{2} \begin{pmatrix} G_t\beta_t \\ G_p\beta_p \end{pmatrix}. \tag{6}$$

Reproduction

The contribution to the next generation of a mating between a male with trait t and a female with preference p is given by

$$W_r(t,p) = \exp\left[-a(p-t)^2\right], \tag{7}$$

where female choosiness a, assumed constant among females, quantifies how much females reject males with a non-preferred trait. We assume weak preference, in line with the previously-described weak selection hypothesis, *i.e.* a being of order ε, with ε small, and that $a > 0$.

Ancestral trait value

The phenotypic evolution in the *focal* species also strongly depends on ancestral trait value t_a, and on the distance between this ancestral value and the trait value displayed in the *local mimicry ring*.

Phenotypic evolution in the *focal* species away from this ancestral trait is limited by developmental as well as selective constraints, specific to the *focal* species. The natural selection exerted on an individual displaying a trait value t then depends on (1) natural selection due to mimetic protection against predation, as well as (2) departure from the ancestral trait value t_a, inducing a selective and developmental cost s. It is thus given by:

$$W_{ns}(t) = W_{pred}(t)\exp\left[-s(t-t_a)^2\right], \tag{8}$$

where W_{pred} is the fitness component due to predation (see Equation (11) below). We assume a selective coefficient s of order ε^2, because we focus on the specific case where selective pressures

due to selective constraints, predation and reproductive interference are of the same order of magnitude (see Appendix 1.1).

Predation depending on the level of mimicry of trait t.

The evolution of the trait t, expressed by males and females from the *focal* species, is strongly influenced by the trait displayed by the individuals from the *local mimicry ring* (mean value $\overline{t}'$). Müllerian mimicry indeed generates positive density-dependent selection (Benson, 1972; Chouteau et al., 2016; Mallet and Barton, 1989), due to predator learning. This density-dependence is non linear and is often modelled as an hyperbolic decrease in mortality (see (Joron and Iwasa, 2005; Llaurens et al., 2013) for example). The density-dependence is modulated by the individual defense level λ, assumed constant among individuals of the *focal* species, shaping predator deterrence: the higher the defense, the quicker predators learn. We note $\overline{\lambda}'$ the mean defense level of an individual in the *local mimicry ring*. The protection gained against predators then depends on the level of resemblance among defended prey, as perceived by predator and the number of individuals sharing the same trait. The level of protection gained by an individual with trait t because of its resemblance with other individuals is given by:

$$\mathcal{D}(t) = \overbrace{\int_{\tau} \lambda N f(\tau) \exp\left[-b(t-\tau)^2\right] \mathrm{d}\tau}^{\substack{\text{protection gained by resemblance} \\ \text{with individuals of the } \textit{focal} \text{ species}}} + \overbrace{\int_{t'} \lambda' N' g(t') \exp\left[-b(t-t')^2\right] \mathrm{d}t'}^{\substack{\text{protection gained by resemblance} \\ \text{with individuals of the } \textit{local mimicry ring} \text{ species}}} , \qquad (9)$$

where N and N' are the densities of individuals in the *focal* species and in the *local mimicry ring*, respectively and $\exp\left[-b(t-\tau)^2\right]$ describes how much predators perceive the trait values t and τ as similar. The predator discrimination coefficient b thus quantifies how much predators discriminate different trait values. We assume that this parameter is of the same order of magnitude as female choosiness a (*i.e* of order ε). f and g are the distribution of traits in the *focal* species and in the *local mimicry ring* species respectively. Assuming that the distribution of traits has a low variance within both the *focal* species and the *local mimicry ring* leads to the following approximation

(see Appendix 1.1):

$$\mathcal{D}(t) \approx \lambda N \exp\left[-b(t-\bar{t})^2\right] + \lambda' N' \exp\left[-b(t-\bar{t}')^2\right]. \tag{10}$$?Dapprox

We note $d \in (0,1)$ the basal predation rate and we assume this parameter to be of order ε, with ε small, in line with the weak selection hypothesis. The impact of predation on the fitness of an individual displaying the trait value t is given by:

$$W_{pred}(t) = 1 - \frac{d}{\mathcal{D}(t)}, \tag{11}$$?Wpred

where $\exp\left[-b(t-\bar{t}')^2\right]$ (resp. $\exp\left[-b(t-\bar{t})^2\right]$) describes how much predators perceive the trait values t and $\bar{t}'$ (resp. $\bar{t}$) as similar.

Cost induced by reproductive interference.

Because males of the *local mimicry ring* may resemble males of the *focal* species, females will suffer from reproductive interference generated by erroneous mating attempts with heterospecific males (see (Gröning and Hochkirch, 2008) for a review of reproductive interference costs). The risk of heterospecific mating depends on the relative densities of heterospecific and conspecific males. The cost of reproductive interference is thus assumed to be density-dependent in the model. We assume a balanced sex-ratio within both the *focal* species and the *local mimicry ring*. However, we also consider the capacity of females to recognize conspecific males using alternative cues (pheromones for example). In the model, the investment of females in interspecific mating interaction is captured by the parameter $c_{RI} \in [0,1]$. This cost of reproductive interference incurred to females can be reduced when female choice is also based on alternative cues differing between mimetic species. Using Equation (1b) in (Yamaguchi and Iwasa, 2013) the fitness of a

female with preference p is modulated by:

$$W_{RI}(p) = \frac{\displaystyle\int_t \overbrace{\frac{N}{N+N'} f(t)}^{\substack{\text{probability of encountering}\\ \text{a conspecific male}\\ \text{with trait } t}} \overbrace{\exp\left[-a(p-t)^2\right]}^{\substack{\text{probability of accepting}\\ \text{a conspecific male}\\ \text{with trait } t}} \mathrm{d}t}{\displaystyle\int_t \frac{N}{N+N'} f(t) \exp\left[-a(p-t)^2\right] \mathrm{d}t + \int_{t'} \underbrace{\frac{N'}{N+N'} g(t')}_{\substack{\text{probability of encountering}\\ \text{an heterospecific male}\\ \text{with trait } t'}} \underbrace{c_{RI} \exp\left[-a(p-t')^2\right]}_{\substack{\text{probability of accepting}\\ \text{an heterospecific male}\\ \text{with trait } t'}} \mathrm{d}t'},$$

(12) ?wRI

where c_{RI} is the strength of RI, assumed of order ε, with ε small, in line with the weak selection hypothesis.

Assuming that the distribution of traits has a low variance within both the *focal* species and the *local mimicry ring* leads as before to the following approximation:

$$W_{RI}(p) = \frac{\exp\left[-a(p-\bar{t})^2\right] N}{\exp\left[-a(p-\bar{t})^2\right] N + c_{RI} \exp\left[-a(p-\bar{t}')^2\right] N'}. \tag{13}$$

?wRIapprox

All variables and parameters used in the model are summed up in Table 1.

Model exploration.

We assume that the *focal* species is ancestrally not in contact with the *local mimicry ring* displaying the ancestral trait t_a. We also assume that mean female preference value is initially equal to mean trait value. At the initial time, we assume that the *focal* species enters in contact with the *local mimicry ring*. The dynamics of trait and preference values then follow Equation (6).

Analytical resolution assuming weak female choosiness ($a = O(\varepsilon)$) and predator discrimination ($b = O(\varepsilon)$). Assuming that a and b are of order ε and s is of order ε^2 (hypothesis H_w), we analytically determine the mean trait and preference values in the *focal* species at equilibrium ($\bar{t}^*$ and $\bar{p}^*$). To identify the conditions enabling advergence toward the *local mimicry ring*, we estimate $|\bar{t}^* - \bar{t}'|$, *i.e.* the phenotypic distance between the mean trait within the *focal* species and the mean trait displayed in the *local mimicry ring*.

Table 1: Description of variables and parameters used in the model assuming a fixed *local mimicry ring*

tab:desc1

Abbreviation	Description
$\overline{t}/\overline{p}$	Mean trait/preference value in the *focal* species
G_t/G_p	Genetic variance of trait t/preference p
C_{tp}	Genetic covariance between trait t and preference p
β_t/β_p	Selection coefficient on trait t/preference p
$\overline{t}'$	Mean trait value in the mimetic community
a	Female choosiness
s	Strength of selective and developmental constraints promoting the ancestral trait value t_a
t_a	ancestral trait value in the focal species
d	Basal predation rate
b	Predator discrimination coefficient
λ	defense level carried out by individuals of the focal species
$\overline{\lambda}'$	Mean defense level of an individual of the local mimicry ring
N/N'	Density of the focal species/local mimicry ring
c_{RI}	Strength of reproductive interference

To estimate how much sexual selection impairs phenotypic advergence toward the *local mimicry ring*, we then compute the discrepancy between trait and preference values in the focal species $|\overline{t}^* - \overline{p}^*|$.

Model exploration assuming strong female choosiness ($a = O(1)$) and predator discrimination ($b = O(1)$). Because the stringency of females choice, as well as the discrimination behavior of predators, are key drivers of the advergence toward the trait displayed in the *local mimicry ring*, we then explore large values of female choosiness and predator discrimination, *i.e.* $a = O(1)$ and $b = O(1)$. Under such assumptions, the effects of predation and reproductive interference on the changes in

the mean trait and preference are of order ε. We also assume that s is of order ε, because if s is of order ε^2 the strength of developmental and selective constraints would be negligible compared with selection due to predation and reproductive interference. Assuming strong female choosiness violates the weak selection hypothesis, because strong female choosiness generates strong sexual selection for males and opportunity cost for females. However, because strong female choosiness leads to higher sexual selection, the discrepancy between preference and trait values ($|\bar{t}^* - \bar{p}^*|$) becomes limited. Therefore sexual selection and opportunity cost are actually weak and we can still estimate the matrix of genetic covariance and assume that the genetic variances of traits and preference are low. However, because of the complexity of the model, under strong female choosiness ($a = O(1)$) and predator discrimination ($b = O(1)$), we cannot analytically determine the mean trait and preference values at equilibrium ($\bar{t}^*$ and $\bar{p}^*$). We then use numerical simulations of Equation (6) to explore cases where a and b are of order 1 and s is of order ε (hypothesis H_s)

By default, we report results assuming (H_w). We also verified that the results stand assuming (H_s) (see Appendix 1.7). When the parameters have the same effect assuming (H_w) or (H_s), we do not provide the effect of parameters assuming (H_s).

Results

We study the evolution of the mean values of trait and preference in the *focal* species, described by Equation (6). When

$$c_{RI} < \frac{N}{aN'}\left(\frac{4bd\overline{\lambda}'N'}{(1+\lambda N+\overline{\lambda}'N')^2} + 4s\right), \tag{14}$$?smallRI

mean trait and preference values converge to the equilibrium values $\bar{t}^*$ and $\bar{p}^*$ with

$$\bar{t}^* = \frac{\frac{2bd\overline{\lambda}'N'}{(1+\lambda N+\overline{\lambda}'N')^2}\bar{t}' + 2st_a - ac_{RI}\frac{N'}{N}\bar{t}'}{\frac{2bd\overline{\lambda}'N'}{(1+\lambda N+\overline{\lambda}'N')^2} + 2s - ac_{RI}\frac{N'}{N}}, \tag{15}$$ {?}

and

$$\bar{p}^* = \bar{t}^* + c_{RI}\frac{N'}{N}(\bar{t}^* - \bar{t}'). \tag{16}$$?pref

These analytical expressions allow us to study the impact of the different evolutionary forces on the level of advergence of the trait displayed in the *focal* species toward the trait exhibited in the *local mimicry ring* ($|\bar{t}^* - \bar{t}'|$).

Otherwise when (14) is not verified the distances between mean trait and preference values in the *focal* and $\bar{t}'$ become very large (not of order 1) (see Appendix 1.5).

Reproductive interference limits advergence toward the local mimicry ring.

Selection exerted by predators favors the advergence of trait in the *focal* species toward the trait exhibited by the *local mimicry ring*. When (14) is verified the level of advergence toward the local mimicry ring is given by:

$$|\bar{t}^* - \bar{t}'| = \frac{2s}{\frac{2bd\bar{\lambda}'N'}{(1+\lambda N+\bar{\lambda}'N')^2} + 2s - ac_{RI}\frac{N'}{N}}|t_a - \bar{t}'|. \tag{17}$$

Hence, if we assume no reproductive interference ($c_{RI} = 0$), we have $|\bar{t}^* - \bar{t}'| < |t_a - \bar{t}'|$, implying that the trait displayed in the *focal* species gets closer to the trait displayed in the *local mimicry ring*: we thus observe different evolutionary outcomes ranging from (a) *mimicry* to (b) *imperfect mimicry*, see Figures 1(a) and 1(b). The mimicry in the *focal* species becomes nearly perfect ($|\bar{t}^* - \bar{t}'|$ close to zero) when the strength of selection due to predation ($2bd\bar{\lambda}'N'/(1 + \lambda N + \bar{\lambda}'N')^2$) is large enough, as compared to the intra-specific constraints (s) (outcome (a) *mimicry* see Figure 1(a)).

However assuming reproductive interference between females from the *focal* species and males from the *local mimicry ring* impairs advergence. When reproductive interference is non null but has a limited strength, satisfying Inequality (14), Equation (17) implies that $\partial|\bar{t}^* - \bar{t}'|/\partial c_{RI} > 0$ (see Appendix 1.7.1). reproductive interference thus increases the gap between the traits displayed in the *focal* species and in *the local mimicry ring*, leading to imperfect mimicry in the *focal* species. Because females' preference generates sexual selection on male traits, reproductive interference promotes phenotypic divergence between the *focal* species and the *local mimicry ring* (see Equation (16)). Thus reproductive interference limits the advergence generated by Müllerian mimicry.

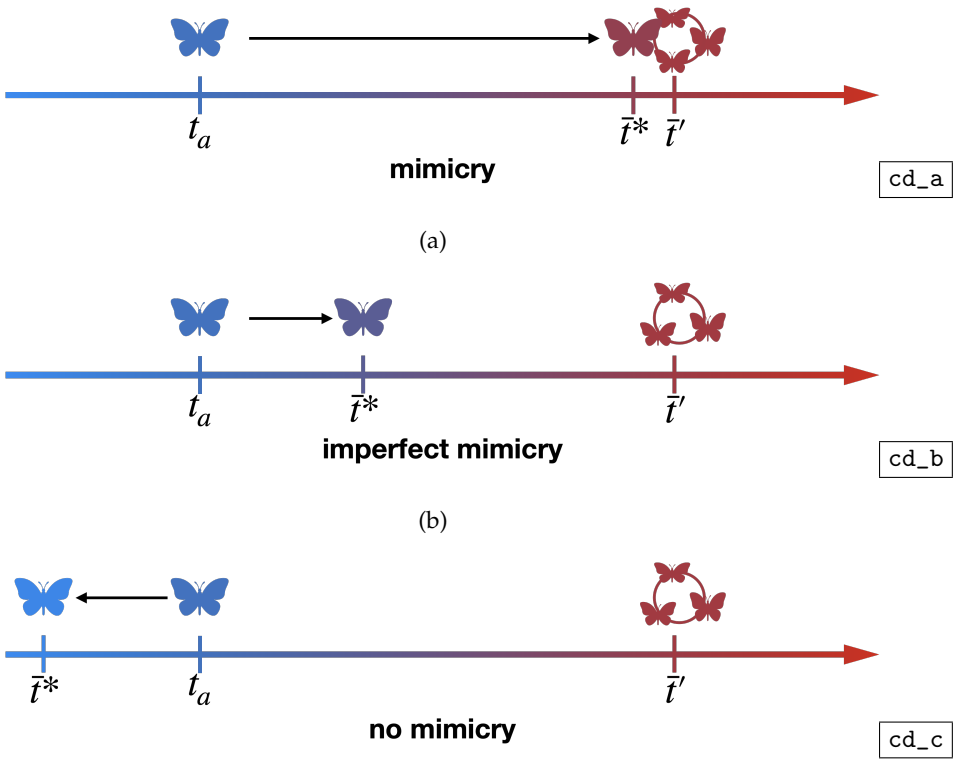

Figure 1: **Illustration of three possible outcomes:** (a) *mimicry*: the value of the trait in the *focal* species $\bar{t}$ becomes very close to the mean value displayed in the *local mimicry ring* $\bar{t}'$, (b) *imperfect mimicry*: the value of the trait in the *focal* species $\bar{t}$ gets closer but stays distant from the mean value displayed in the *local mimicry ring* $\bar{t}'$, (c) *no mimicry*: the value of the trait in the *focal* species $\bar{t}$ diverges away from the mean value displayed in the *local mimicry ring* $\bar{t}'$.

cd

However, when the cost associated with reproductive interference crosses a threshold, *i.e.* when

$$\frac{N}{aN'}\frac{4bd\bar{\lambda}'N'}{(1+\lambda N+\bar{\lambda}'N')^2} \leq c_{RI} < \frac{N}{aN'}\left(\frac{4bd\bar{\lambda}'N'}{(1+\lambda N+\bar{\lambda}'N')^2}+4s\right), \tag{18}$$ {?}

then

$$|\bar{t}^* - \bar{t}'| > |t_a - \bar{t}'|. \tag{19}$$ {?}

When assuming such an elevated cost of RI, imperfect mimicry is thus no longer observed, and reproductive interference rather promotes a strong divergence of the trait in the *focal* species (see

Figure 1(c) for an illustration).

When inequality (14) is not satisfied, the phenotypic distance between the *focal* species and the *local mimicry ring* becomes very large. This very large divergence is biologically unrealistic but suggests that reproductive interference can promote phenotypic divergence between defended species living in sympatry. This unrealistic divergence stems from the weak female choosiness ($a = O(\varepsilon)$) assumed: since females have broad preference (because a is low), females almost always accept heterospecific males, except when the difference between female preference and the trait displayed in the *local mimicry ring* is very high. Reproductive interference promotes female preference that limits fitness costs due to RI, and therefore promotes a large distance between female preference value and the value of the trait displayed in the *local mimicry ring*.

Relaxing the weak preference and predator discrimination hypothesis, *i.e.* assuming that $a = O(1)$ and $b = O(1)$, confirms that reproductive interference limits mimicry in the *focal* species. However, in this case, when a strong divergence is favored, this divergence becomes high but stays of order $O(1)$ (see Appendix 1.6). Indeed, as female choosiness is strong, this divergence strongly reduces fitness cost due to reproductive interference. Therefore stabilizing constraints on the trait in the *focal* species become more important than RI, thereby preventing very large divergence.

Strict female choosiness and moderate predator discrimination favor convergence of warning traits, despite reproductive interference.

The evolution of the trait in the *focal* species is shaped by two antagonistic evolutionary forces, generated by reproductive interference and Müllerian mimicry, respectively. Reproductive interference indirectly limits the advergence toward the *local mimicry ring* by impacting females' preference. Therefore, females' choosiness a may be a key feature to understand the evolution of the trait in the *focal* species. The selection exerted by predation also depends on animal behavior through predators' learning. We thus investigate the impact of the strength of female choosiness a and of predator discrimination coefficient b on the evolution of the warning trait, allowing

strong values of a and b (*i.e.* assuming (H_s)).

When the female choosiness is low, the selection promoting divergence generated by reproductive interference is limited. Indeed, females are not choosy and tend to accept all encountered males, including heterospecific males, whatever the direction of their preference. The difference in fitness cost due to reproductive interference between females with different preferences is then low, leading to poor selection due to reproductive interference. With a higher level of female choosiness, fitness cost due to reproductive interference depends more on the direction of preference, leading to higher selection caused by reproductive interference. Therefore, when the value of female choosiness (a) increases from 0 to 1, mimicry becomes less likely to evolve.

By contrast, Figure 2 highlights that mimicry becomes more likely as female choosiness a takes values above 1. Higher levels of female choosiness allow females to accurately distinguish males from their own species from individuals from the local mimicry ring. Accurate choice by females allows a quasi similarity of the traits of the focal species and of the local mimicry ring, without implying heterospecific mating, relaxing selection promoting divergence generated by reproductive interference. The evolutionary outcome is also impacted by selection exerted by predation. The predation rate depends on predators discrimination coefficient b, modulating their capacity to differentiate traits displayed in different mimetic species. When predators tend to generalize (when b is approximately close to 0) there is no mimicry because there is no selection promoting similarity between the *focal* species and the *local mimicry ring*. When b is greater than 0 but approximately similarly lower than 5, the higher discrimination of predators reduces the distances between the average traits displayed in the *focal* species and the *local mimicry ring* (Figure 2), leading to more accurate mimicry (see Appendix 1.7.2 for more detail). Surprisingly, when predator discrimination increases above a certain threshold, increased discrimination no longer promotes accurate mimicry (see sharp transition between mimicry (red) and no mimicry (blue) in Figure 2). When b is high, individuals from the *focal* species benefit from protection gained by mimicry only when they look very similar to the individuals of the local mimicry ring. Reproductive interference makes such high similarity too costly, and therefore divergence of the

trait in the *focal* species becomes promoted when predator discrimination is too high (Figure 2).

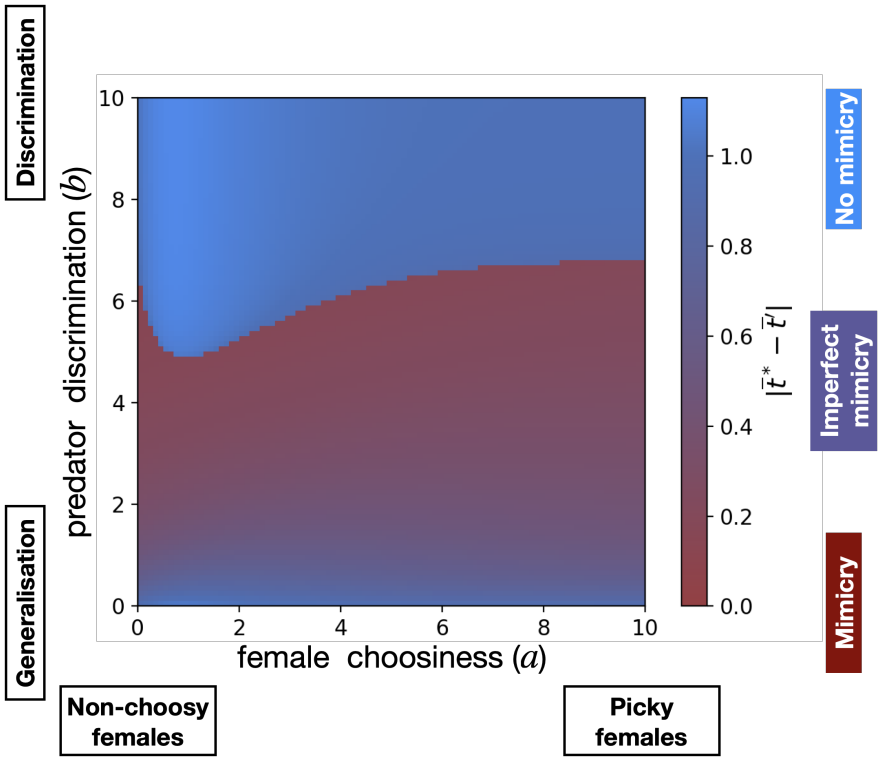

Figure 2: **Influence of the predator discrimination b and of the strength of female choosiness a on the phenotypic distance between the *focal* species and the *local mimicry ring*.** The plot reports values generated by numerical simulations performed using parameters values of the (H_s) assumption. The parameter range generating *mimicry*, *imperfect mimicry* and *no mimicry* are shown in red, purple and blue respectively. We assume: $G_t = 0.01$, $G_p = 0.01$, $c_{RI} = 0.002$, $d = 0.02$, $\lambda = 0.1$, $N = 20$, $\overline{\lambda}' = 0.1$, $N' = 20$, $s = 0.005$, $t_a = 0$, $\bar{t}' = 1$.

ab

Reproductive interference limits mimicry in species with low density.

The defense level of the *focal* species, *i.e.* λN, is likely to impact the level of trait divergence. Without RI, $\partial|\bar{t}^* - \bar{t}'|/\partial\lambda N > 0$ indicates that the defense level in the *focal* species increases divergence from the trait displayed in the *local mimicry ring*. As expected, advergence toward the warning trait is thus more likely to happen when the *focal* species is weakly defended (λN

small). Indeed, individuals from weakly defended species gain a limited protection from conspecific individuals and have a great advantage gained from mimicry to the local community of well-defended species. By contrast, individuals of a well-defended species get protection from their conspecifics, and therefore the selective pressure favoring similarity to the *local mimicry ring* is weaker. In well-defended species, developmental and selective constraints promoting the ancestral trait t_a exceed selection favoring similarity and promote the persistence of traits in the *focal* species distinct from the *local mimicry ring*. To understand the interaction between the two components of the defense level, we then compared the effect of the density N and of the individual defense level λ of the focal species, for different costs of choosiness (Figure 3). Without reproductive interference ($c_{RI} = 0$), yellow defense level λN isolines in Figure 3(a) show that the phenotypic distance between the *focal* species and the *local mimicry ring* only depends on the product λN (see). Moreover Figure 3(a) confirms that low defense level λN promotes mimicry in the *focal* species.

By contrast, assuming reproductive interference ($c_{RI} > 0$), Figures 3(b)-(c) show that the evolutionary outcome depends more on the individual defense level than on the density of the *focal* species. The advergence toward the trait displayed in the *local mimicry ring* is observed when the individual defense level is low (λ approximately lower than 0.1) and when the density of the *focal* species is sufficiently large (N approximately greater than 5). In this case, the defense level of the *focal* species (λN) is low, the protection gained by positive frequency-dependent selection within species is low, and the advergence toward the *local mimicry ring* is thus strongly promoted. Surprisingly, this advergence is impaired for similar values of defense level, when the density of the focal species is low (N approximately lower than 5). When the density of the *focal* species is low, females pay higher fitness costs due to RI, because they encounter more often heterospecific than conspecific males. Altogether, our results suggest that advergence of the warning traits is likely to happen for low level of individual defense in the *focal* species (*i.e.* Batesian ($\lambda = 0$) or quasi-Batesian ($\lambda > 0$ but small) mimicry) and when the density of the *focal* species is high.

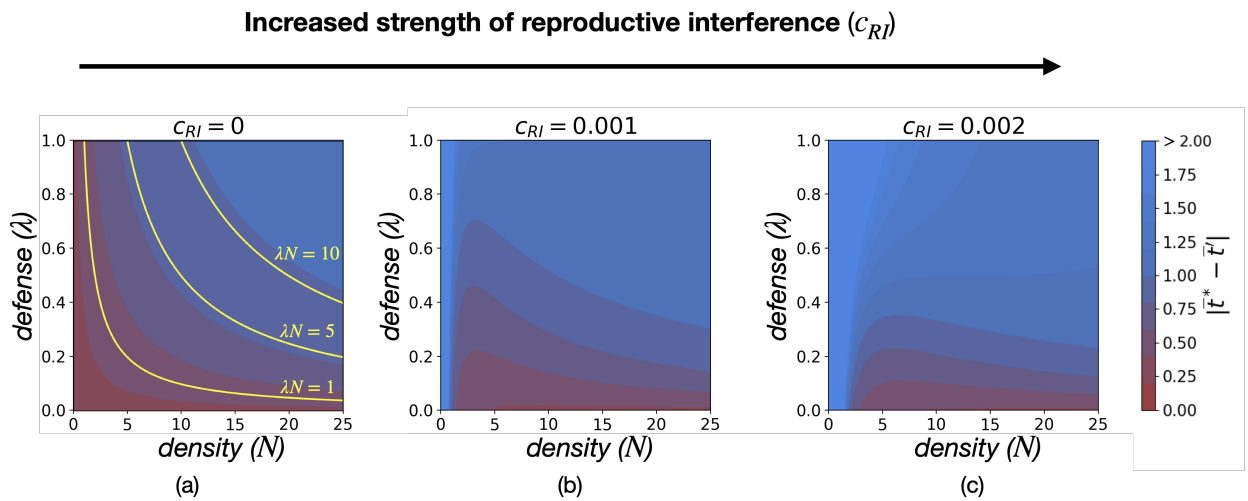

Figure 3: **Influence of the density of the *focal* species N and of individual defense level in the *focal* species λ on the phenotypic distance between the *focal* species and the *local mimicry ring*, for different strengths of reproductive interference c_{RI}.** The plot reports values generated by the analytic approximation assuming (H_w). The parameter ranges generating *mimicry*, *imperfect mimicry* and *no mimicry* are shown in red, purple and blue, respectively. Phenotypic distances greater than 2 are shown in blue. Yellow lines indicate equal levels of defense level in the *focal* species λN. Different values of strengths of reproductive interference are assumed: (a) $c_{RI} = 0$, (b) $c_{RI} = 0.001$, (c) $c_{RI} = 0.002$. We assume: $a = 0.01$, $d = 0.05$, $b = 0.01$, $\overline{\lambda}' = 0.1$, $N' = 20$, $s = 0.00005$, $t_a = 0$, $\bar{t}' = 1$.

wd

Evolution of warning traits within two interacting species

Method

Because reproductive interference may impact the direction of advergence, and because ancestral traits that might differ among species may influence the evolution of traits, we build an extension of the previous model by assuming two sympatric species, whose traits can evolve. This two-species model allows investigating the eco-evolutionary dynamics of trait convergence. We thus follow the evolution of traits (t_1 and t_2 in species 1 and 2, respectively) and female choosiness (p_1

and p_2 in species 1 and 2, respectively). Because the two species are assumed to be fully sympatric, individuals from both species face the same community of predators, and can encounter each others. The evolution of trait and preference in both species are thus shaped by both (1) Müllerian mimicry and (2) reproductive interference caused by heterospecific mating.

Assuming that traits and preferences have an autosomal polygenic basis with additive effects in both species, the change in the mean values of traits $(\bar{t}_1, \bar{t}_2)$ and preferences $(\overline{p}_1, \overline{p}_2)$ can be approximated using:

$$\begin{pmatrix} \Delta\bar{t}_i \\ \Delta\overline{p}_i \end{pmatrix} = \frac{1}{2} \begin{pmatrix} G_{t_i} & C_{t_i p_i} \\ C_{t_i p_i} & G_{p_i} \end{pmatrix} \begin{pmatrix} \beta_{t_i} \\ \beta_{p_i} \end{pmatrix} \approx \frac{1}{2} \begin{pmatrix} G_{t_i}\beta_{t_i} \\ G_{p_i}\beta_{p_i} \end{pmatrix}, \tag{20}$$

where for $i \in \{1, 2\}$ the variables β_{t_i} and β_{p_i} describe the selective forces acting on the traits and preferences t_i and p_i (defined in Appendix 2.2). G_{t_i} and G_{p_i} are the additive genetic variances of t_i and p_i and $C_{t_i p_i}$ is the additive genetic covariance between t_i and p_i. As in the previously described model, following (Iwasa et al., 1991), we assume that G_{t_i} and G_{p_i} are positive constants maintained by an equilibrium between selection and recurrent mutations. As we already showed (see Appendix 1.3), the additive genetic covariance $C_{t_i p_i}$ is small in comparison with G_{t_i} and G_{p_i}, allowing us to approximate the change in the mean values of trait and preference as done in (20).

Female choosiness (a_1 and a_2), strength of selective and developmental constraints (s_1 and s_2), ancestral trait (t_{a1} and t_{a2}), defense level (λ_1 and λ_2) carried out by individuals, as well as density (N_1 and N_2) can differ between species 1 and 2. All variables and parameters used in the two-population model are summed up in the supplementary Table A1.

Model exploration.

To specifically test the effect of species interactions on trait convergence, we assume the two species to be initially isolated and explore trait evolution when they become sympatric. We also assume the initial mean female preferences value to equal ancestral trait values within each species. The dynamics of the mean trait and preference values when both species become in contact are then given by Equation (20).

Exploration assuming weak female choosiness ($a_1 = O(\varepsilon)$ and $a_2 = O(\varepsilon)$) and predator discrimination ($b = O(\varepsilon)$) (Hypothesis (H_w)). When we assume that a_1, a_2 and b are of order ε and s is of order ε^2, we can analytically determine the mean traits and preferences values at equilibrium in most cases. In the few remaining cases, we use numerical analyses to estimate these values (see Appendix 2.4). We note $\overline{t}_1^*, \overline{t}_2^*, \overline{p}_1^*$ and $\overline{p}_2^*$ the mean traits and preferences at equilibrium. We follow the quantity $|\overline{t}_1^* - \overline{t}_2^*|$, *i.e.* the mean phenotypic distance between both species at equilibrium. To determine the direction of advergence, we check whether the trait values observed at equilibrium (*i.e.* $\overline{t}_1^*$ and $\overline{t}_2^*$) are closer to the ancestral trait value of species 1 or of species 2 (t_{a1} or t_{a2} respectively).

Exploration assuming strong female choosiness ($a_1 = O(1)$ and $a_2 = O(\varepsilon)$) and predator discrimination ($b = O(1)$) (Hypothesis $((H_s))$). Similarly to the previous model exploration, we use numerical simulations to study cases where female choosiness and predator discrimination are strong ($a_1 = O(1)$, $a_2 = O(1)$, $b = O(1)$ and $s = O(\varepsilon)$).

As in the exploration of the previous model, by default we report results assuming (H_w) and check the validity of these results when assuming (H_s) (see Appendix 2.5).

Results

Reproductive interference may reverse the direction of advergence.

As previously unraveled, reproductive interference may limit the convergence of warning traits, depending on the level of defense and on the density of the two mimetic species (Figure 3(c)). By studying the two-species model, we can also investigate how reproductive interference may influence the direction of advergence, depending on the relative levels of defense of the two species, generated by their densities and individual strength of defense ($\lambda_1 N_1$ and $\lambda_2 N_2$, respectively). The fitness costs caused by reproductive interference then also differ between the two species, depending on their relative abundances, leading to unbalanced selective pressures on trait evolution in the two species: females from the rarest species suffer more from RI, because

they encounter heterospecific more often than conspecific males.

To investigate how the relative defense levels of the two species affect the direction of advergence, we study the phenotype at equilibrium in both species, for different values of the two components of the defense level of species 1: the individual defense level (λ_1) and the density (N_1). Here we assumed that species 2 is already well protected ($\lambda_2 = 0.1$, $N_2 = 10$).

When assuming no reproductive interference ($c_{RI} = 0$), species traits converge toward the ancestral trait t_a initially displayed in the best defended species. In Figures 4(a) and 4(b), individuals from the poorly defended species 1 (*i.e.* when $\lambda_1 N_1$ is low) get weak protection from conspecific individuals and thus have a greater advantage to look similar to individuals of species 2. The more species 1 is defended, *i.e.* the greater $\lambda_1 N_1$ is, the closer its mean trait value is to the ancestral trait value t_{a1} (see Figure 4(a)). Such increase in the defense level of species 1 also impacts the evolution of trait in the sympatric species 2 (see Figure 4(b)): when the individual defense level in species 1 (λ_1) is below a threshold, the more individuals from species 1 are protected, the more the mean trait value in species 2 moves away from its ancestral trait (t_{a2}). Surprisingly, above this threshold, the better protected species 1 is, the closer the mean trait value in species 2 gets to its ancestral trait value (t_{a2}). The weak discrimination capacities of predators assumed favors such evolution of divergent traits. Individuals from species 2 may thus gain some protection from species 1 even with a poor resemblance. When species 1 is highly protected (high $\lambda_1 N_1$), the level of protection gained by individuals of species 2 because of their resemblance with individuals of species 1 ($\lambda_1 N_1 \exp\left[-b(\bar{t}_1 - \bar{t}_2)^2\right]$) is high, even when individuals of species 2 display poorly mimetic trait, close to the ancestral trait value ($\bar{t}_2 = t_{a2}$). The selective and developmental constraints within species 2 then keep the trait in species 2 close to its ancestral trait value t_{a2}.

When assuming positive strength of reproductive interference ($c_{RI} > 0$), the trait value of species 1 almost never converges toward the trait value initially displayed in species 2 (t_{a2}). On the contrary, individuals of species 2 can mimic individuals of species 1 (see blue zone in Figure 4(d)), when the defense level of individuals of species 1 is high and when species 1 is rare. Because individuals from both species are well defended (high λ_1 and λ_2), individuals of both

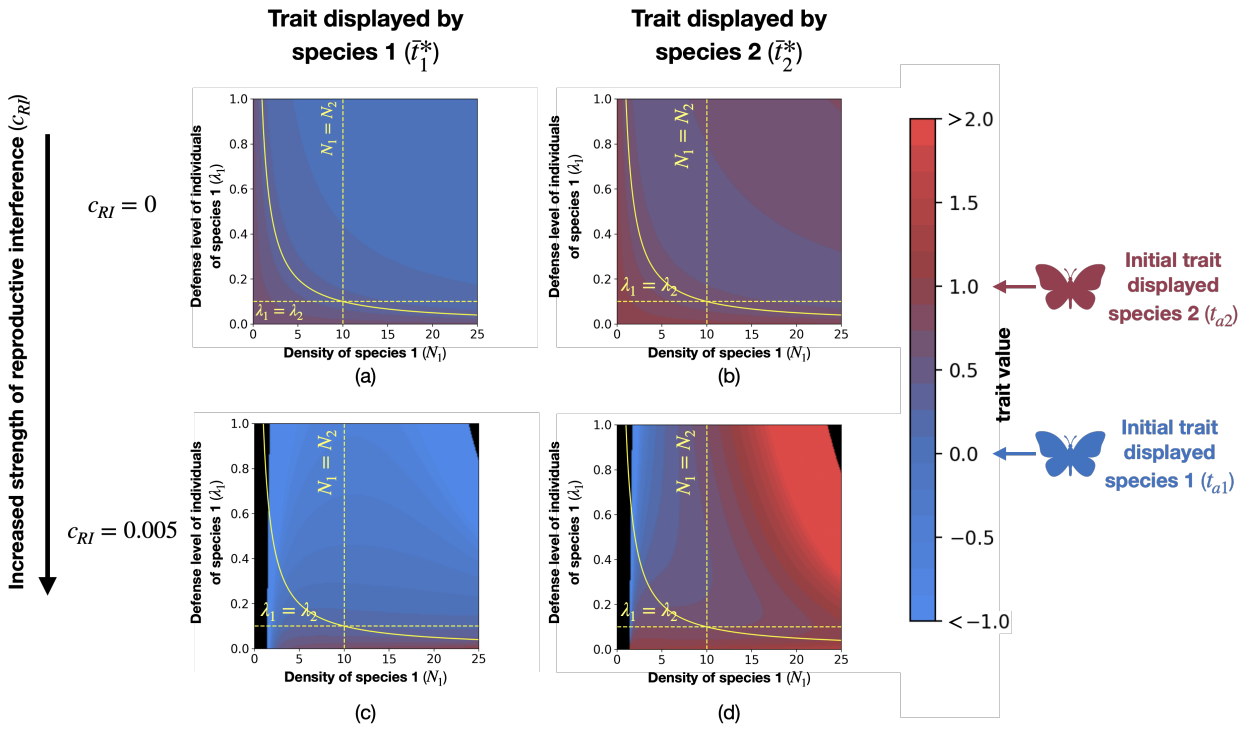

Figure 4: **Influence of the density and of the individual defense level in species 1 (N_1 and λ_1) on the traits displayed in both species, for different strengths of reproductive interference (c_{RI}).** Plots report values obtained with the analytic approximation, assuming (H_w). Mean trait values can become very large (black zone). Trait values greater than 2 (resp. lower than -1) are shown in red (resp. blue). The yellow solid line shows the case where both species have the same level of defense ($\lambda_1 N_1 = \lambda_2 N_2$). Below (resp. above) this line species 1 has a lower (resp. higher) level of defense than species 2. Different values of strengths of reproductive interference are assumed: (a) and (b) $c_{RI} = 0$, (c) and (d) $c_{RI} = 0.005$. We assume: $a_1 = a_2 = 0.01$, $d = 0.05$, $b = 0.01$, $\lambda_2 = 0.1$, $N_2 = 10$, $s_1 = s_2 = 0.000005$, $t_{a1} = 0$, $t_{a2} = 1$.

t1_t2

species benefit from looking similar. However, when species 1 is rarer, this leads to an increased cost of RI in species 1, inhibiting convergence towards the ancestral trait value displayed in the alternative species (t_{a2}) (see Figure 4(c)). Since predation pressure promotes convergence of traits of both species, the mean trait in species 2 becomes closer to species 1 ancestral trait value t_{a1}. Surprisingly, such advergence also happens when individuals of species 2 are more

defended than individuals from species 1, *i.e.* $\lambda_2 N_2 > \lambda_1 N_1$ (see blue zones in Figures 4(c) and (d) below the yellow solid line). By contrast, when the density in species 1 exceeds the density in species 2, individuals from both species exhibit traits close to their ancestral traits. As previously explained, both species are well-protected and then gain little from mimicry. However, the phenotypic distance between the two species is higher than in the previous case, because reproductive interference further promotes trait dissimilarity (see Figure 4).

Our results highlight that reproductive interference impacts the evolution of warning traits, and may even reverse the direction of advergence, depending on the relative abundances and defense levels of sympatric species.

Ancestral trait values in interacting species strongly modulate phenotypic divergence driven by reproductive interference.

Our previous results highlight that reproductive interference limits the convergence of warning traits. This effect is also observed in the model investigating the evolution of traits in two interacting species. However, the effect of reproductive interference on trait divergence strongly depends on the ancestral trait values initially displayed in the two species in the absence of ecological interactions (t_{a1} and t_{a2}). When these ancestral trait values differ, an increase in strength of reproductive interference leads to a progressive increase in the phenotypic distance between both species (see Figure 5).

Surprisingly, when the ancestral trait values are the same in both species ($t_{a1} = t_{a2}$), an increase in the strength of reproductive interference (c_{RI}) has no effect on the phenotypic distance between both species, as long as this cost of reproductive interference remains below a threshold (see Figures 6(a) and 6(b)). This effect is observed assuming weak (H_w) or strong (H_s) female choosiness and predator discrimination.

However, when the strength of reproductive interference (c_{RI}) is greater than this threshold, assuming weak female choosiness and predator discrimination (H_w), the phenotypic distance between both species becomes instantaneously very large, while their initially displayed ancestral

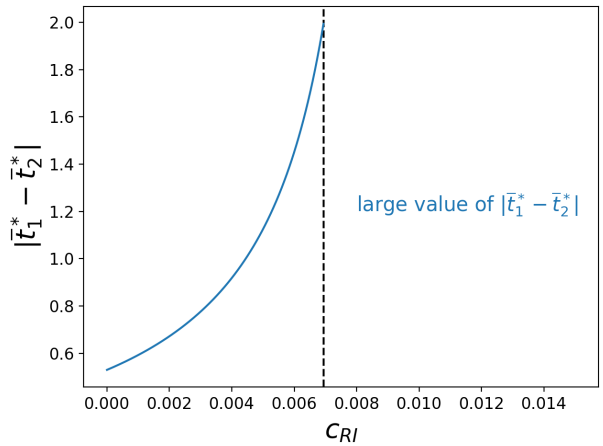

Figure 5: **Influence of the strength of reproductive interference c_{RI} on the phenotypic distances between the two species, when they have different ancestral traits ($t_{a1} \neq t_{a2}$).** The plot reports values obtained by the analytic approximation assuming (H_w). We assume: $a_1 = a_2 = 0.01$, $d = 0.02$, $b = 0.01$, $\lambda_1 = \lambda_2 = 0.1$, $N_1 = N_2 = 10$, $s_1 = s_2 = 0.000005$, $t_{a1} = 0$, $t_{a2} = 1$.

trait values t_{a1} and t_{a2} are equal. A similar trend is observed when female choosiness and predator discrimination are strong (H_s): the phenotypic distance is null when the strength of reproductive interference remains below a threshold, but it quickly increases to a high value when the strength of reproductive interference crosses the threshold (see Figure 6(b)).

Our results highlight that the ancestral trait values strongly modulate the effect of reproductive interference on the convergence of warning traits. Surprisingly, drastic divergence might be promoted by a strong cost of RI, even when the optimal phenotypes are the same in the two interacting species.

Discussion

Reproductive interference leads to unexpected evolution of warning trait

Our model shows that reproductive interference limits the convergence of warning traits in defended species living in sympatry. The effect of reproductive interference strongly depends on

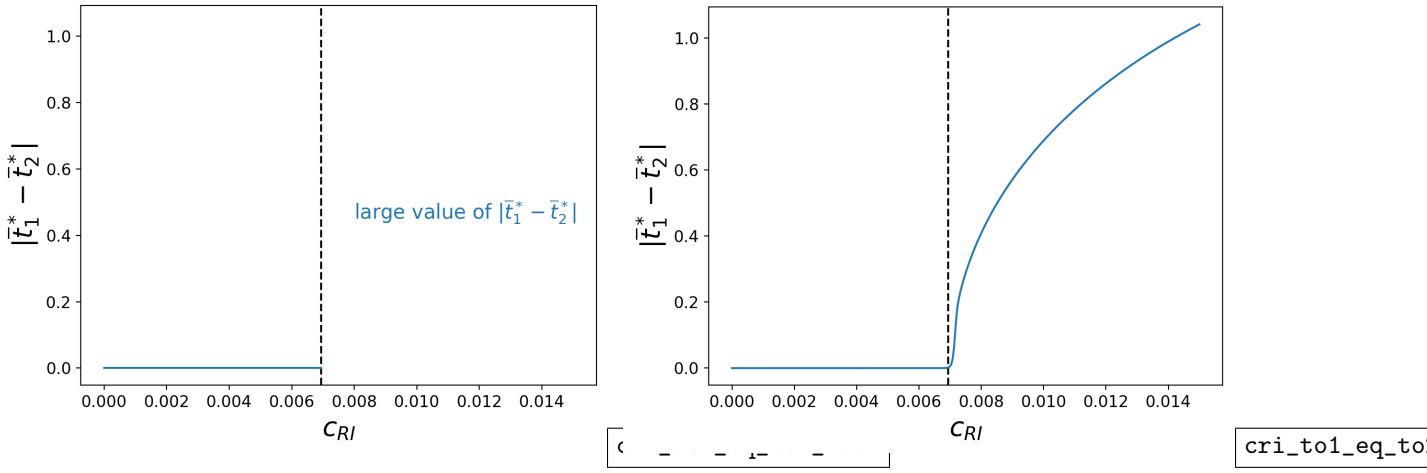

(a) (b)

Figure 6: **Influence of the strength of reproductive interference c_{RI} on the phenotypic distances between the two species when they share the same ancestral traits interaction ($t_{a1} = t_{a2}$), assuming (a) (H_w) weak or (b) (H_s) strong female choosiness and predator discrimination.** Plots report values obtained by (a) the analytic approximation assuming (H_w) and (b) numerical simulations to use parameters values corresponding to (H_s) assumption. Different values of female choosiness, predator discrimination coefficient and strength of selective and developmental constraints are assumed : (a) $a = 0.01, b = 0.01$ and $s = 0.00005$, (b) $a = 1, b = 1$ and $s = 0.005$. We assume: $G_t = 0.01$, $G_p = 0.01$, $d = 0.02$, $\lambda_1 = \lambda_2 = 0.1$, $N_1 = N_2 = 10$, $t_{a1} = t_{a2} = 1$.

the relative abundances of interacting species, leading to surprising evolutionary outcomes. For example, in rare defended species, selection favoring mimicry towards the local community of defended species is expected to be strong. Nevertheless, our model shows that the elevated costs of reproductive interference prevents the evolution of mimicry in the rarest species, because females then encounter much more heterospecific than conspecific males.

Our results thus shed some light not only on the persistence of distinct warning traits within local communities of defended species in the wild, but also on the emergence of these distinct warning traits in the first place. Mimetic diversity is a apparent paradox but several hypotheses have been suggested to promote the persistence of different warning signals, including for

instance the segregation of predators within microhabitats (Beccaloni, 2008; Devries et al., 1999; Elias et al., 2008; Willmott et al., 2017). The spread of distinct warning traits has then frequently been shown to be promoted by demographic stochasticity, as in shifting balance models (Mallet and Joron, 1999; Sherratt, 2006) or in other models combining predator behaviours, such as neophobia, to stochastic effects (Aubier and Sherratt, 2015). However, these models do not provide any selective mechanism explaining the emergence of warning signal with different levels of divergence, contributing to mimetic diversity. By contrast, reproductive interference selects for different levels of divergence in warning traits, and could be a major driver of the diversity of mimetic traits. Note that other mechanisms may generated gradual departure from the ancestral trait value and may also contribute to the diversity of mimetic traits: the evolution of aposematic signals in defended species away from those exhibited in Batesian mimics has been theoretically shown to be promoted (Franks et al., 2009). Artificial modification of the warning trait of mated females has also been demonstrated to reduce harassment by males in the butterfly *H. erato*, and would therefore allow them to lay more eggs, suggesting that evolution of slightly divergent trait could be promoted in females (Merrill et al., 2018).

Reproductive interference may particularly promote the emergence and persistence of a distinct warning trait in low-density populations of warning species coming in contact with a local mimicry ring that exhibits a different warning trait. Nevertheless, our model does not take into account the dynamics of population density, and therefore ignores the extinction risk of low-density populations. Such non-mimetic populations with low density might nevertheless persist in the wild, when the level of individual defense is sufficiently high.

Our model also brings new insights to the ecological processes driving the direction of advergence in warning traits. In the absence of RI, warning traits are expected to evolve in the less defended species (*e.g.* low density populations and/or low level of individual defense) and become mimetic of better-defended species living in sympatry (Balogh and Leimar, 2005; Franks and Sherratt, 2007). When considering the costs of reproductive interference, however, this general trend no longer holds, because warning traits in the most abundant species can evolve toward

the warning trait of the less abundant one.

Our model therefore highlights the interplay between mutualism and reproductive interference in sympatric species, which determines the strength and the direction of advergence of traits involved in these ecological interactions.

The evolution of imperfect mimicry

Our results suggest that reproductive interference alone is unlikely to promote imperfect mimicry, in contradiction with previous predictions (Pfennig and Kikuchi, 2012). When sympatric species share the same ancestral trait, we indeed observe either perfect mimicry or strong trait divergence, depending on the strength of reproductive interference. In our model, imperfect mimicry is observed only when interacting species have different ancestral traits. The contrasted developmental and selective constraints underwent by the different species may thus play an important role in imperfect mimicry. These different constraints are likely strongly correlated with the phylogenetic distances between species: closely-related species are likely to share same genetic basis and developmental pathway leading to the warning trait and to also share similar environments, due to niche conservatism (Chazot et al., 2014; Elias et al., 2008; Joshi et al., 2017). Our results suggest that imperfect mimicry could not be promoted among closely-related species experiencing high levels of reproductive interference but limited differences in ancestral traits. Imperfect mimicry may rather be observed between phylogenetically distant species, subject to more strikingly different developmental and selective constraints, where reproductive interference might be more limited. Distantly related species indeed might have diverged in other traits, facilitating mate recognition through different cues.

How important are developmental and selective constraints in the evolution of warning trait?

Estimating the level of developmental and selective constraints potentially shaping the evolution of warning traits is not straightforward. Genetic studies, reviewed in Joron et al. (2006), show that *Heliconius* species share the same 'toolkit' of genes, repeatedly recruited during both convergent and divergent evolution of warning traits within and between species. This important lability in color patterns observed in this genus suggests a limited level of developmental constraints, facilitating the evolution of mimicry, even between species from different sub-clades within the genus (Hines et al., 2011). By contrast, in butterflies from the tribe ithomiines, a strong phylogenetic signal on the warning trait is observed (Chazot et al., 2014; Elias et al., 2008), suggesting that developmental and selective constraints may limit the evolution of mimicry among distantly related species.

The level of developmental constraints and reproductive interference ~~that~~ are both linked to the phylogenetic distances among species and are interacting factors shaping the mutualistic interactions between defended species living in sympatry. The direction and strength of convergent evolution is thus not entirely defined by relative densities and levels of defense, but also by the evolutionary history of interacting species.

Evolution of female preferences limiting the reproductive interference costs generated by mimicry

Our results show the evolution of close similarity between species, despite the costs of reproductive interference. When female choosiness is high, successful species recognition might occur without decreasing the protection brought by mimicry. Such situation arises when predators largely generalize, and therefore do not discriminate imperfect mimics. Such differences in the discrimination of color patterns between prey and predators are frequently observed in the wild.

For instance, Llaurens et al. (2014) showed that the variations in color pattern between co-mimetic species from the distantly related genus *Heliconius* and *Melinaea* might be better perceived by the *Heliconius* butterflies themselves rather than by avian predators. The evolution of visual perception in females could also enhance species discrimination without impairing mimicry. The evolution of vision in females from the *Heliconius* butterflies indeed coincides with the evolution of the yellow pigments 3-OH-kinurenin displayed on their wings (Bybee et al., 2012). The evolution of high discrimination capacities in mimetic prey, as well as the evolution of mating cue undetected by predators could thus limit the cost of reproductive interference in mimetic prey. In butterflies, mate choice indeed often relies on pheromones that may strongly differ among closely-related mimetic species (Darragh et al., 2017; González-Rojas et al., 2020). Micro-habitat differences among mimetic species may also allow reducing heterospecific encounters while still enjoying the benefit of mimicry by sharing the same predator community (Estrada and Jiggins, 2002). In three *Morpho* butterfly species displaying local convergence in wing patterns (Llaurens et al., 2021), temporal segregation in patrolling activity has been observed between species sharing similar color patterns (Le Roy et al., 2020), which may strongly limit heterospecific rivalry.

The levels of reproductive interference among mimetic species might thus be modulated by the evolution of the converging traits themselves, as well as the evolution of other traits involved in species interactions.

Conclusion

Our analytical and numerical results highlight the role of reproductive interference in the evolution of warning traits. They confirm that reproductive interference limits the convergence of warning trait promoted by mutualistic interactions. Surprisingly, reproductive interference can change the direction of the advergence of warning trait when the species densities are unbalanced. Our results also suggest that reproductive interference alone cannot explain imperfect mimicry, highlighting the role of ancestral traits as well as developmental and selective con-

straints in the evolution of imperfect mimicry.

Data Availability

Codes are available online: github.com/Ludovic-Maisonneuve/limits-of-ev-conv

Acknowledgments

LM would like to thank Dorian Ni for feedbacks on the mathematical part of the study. LM and VL would like to thank Charline Pinna and the whole 'Evolution and Development of Phenotypic Variations' team for stimulating discussions on the evolution of the warning traits. The authors would like to thank the ANR SUPERGENE (ANR-18-CE02-0019) for funding the PhD of LM, and the Emergence program from Paris city council for supporting the team of VL. This work was also supported by the Chair "Modélisation Mathématique et Biodiversité" of VEOLIA- Ecole Polytechnique-MNHN-F.X.

Conflict of interest disclosure

The authors of this preprint declare that they have no conflict of interest with the content of this article.

References

Arias, M., le Poul, Y., Chouteau, M., Boisseau, R., Rosser, N., Théry, M., and Llaurens, V. (2016). Crossing fitness valleys: empirical estimation of a fitness landscape associated with polymorphic mimicry. Proceedings of the Royal Society B: Biological Sciences, 283(1829):20160391.

Aubier, T. G. and Sherratt, T. N. (2015). Diversity in müllerian mimicry: The optimal predator sampling strategy explains both local and regional polymorphism in prey. Evolution, 69(11):2831–2845.

Balogh, A. C. and Leimar, O. (2005). Müllerian mimicry: an examination of fisher's theory of gradual evolutionary change. Proceedings of the Royal Society B: Biological Sciences, 272(1578):2269–2275.

Barton, N. H. and Turelli, M. (1991). Natural and sexual selection on many loci. Genetics, 127(1):229–255.

Beccaloni, G. (1997). Ecology, natural history and behaviour of ithomiine butterflies and their mimics in ecuador (lepidoptera: Nymphalidae: Ithomiinae). Tropical Lepidoptera, 8:103–124.

Beccaloni, G. W. (2008). Vertical stratification of ithomiine butterfly (Nymphalidae: Ithomiinae) mimicry complexes: the relationship between adult flight height and larval host-plant height. Biological Journal of the Linnean Society, 62(3):313–341.

Benitez-Vieyra, S., de Ibarra, N. H., Wertlen, A. M., and Cocucci, A. A. (2007). How to look like a mallow: evidence of floral mimicry between turneraceae and malvaceae. Proceedings of the Royal Society B: Biological Sciences, 274(1623):2239–2248.

Benson, W. W. (1972). Natural selection for mullerian mimicry in heliconius erato in costa rica. Science, 176(4037):936–939.

Boussens-Dumon, G. and Llaurens, V. (2021). Sex, competition and mimicry: an eco-evolutionary model reveals how ecological interactions shape the evolution of phenotypes in sympatry. Oikos, in press.

Briolat, E. S., Burdfield-Steel, E. R., Paul, S. C., Rönkä, K. H., Seymoure, B. M., Stankowich, T., and Stuckert, A. M. M. (2019). Diversity in warning coloration: selective paradox or the norm? Biological Reviews, 94(2):388–414.

Brown, W. L. and Wilson, E. O. (1956). Character displacement. Systematic Zoology, 5(2):49–64.

Bybee, S. M., Yuan, F., Ramstetter, M. D., Llorente-Bousquets, J., Reed, R. D., Osorio, D., and Briscoe, A. D. (2012). Uv photoreceptors and uv-yellow wing pigments in heliconius butterflies

allow a color signal to serve both mimicry and intraspecific communication. The American Naturalist, 179(1):38–51. PMID: 22173459.

Chazot, N., Willmott, K. R., Santacruz Endara, P. G., Toporov, A., Hill, R. I., Jiggins, C. D., and Elias, M. (2014). Mutualistic mimicry and filtering by altitude shape the structure of andean butterfly communities. The American Naturalist, 183(1):26–39. PMID: 24334733.

Chouteau, M., Arias, M., and Joron, M. (2016). Warning signals are under positive frequency-dependent selection in nature. Proceedings of the National Academy of Sciences, 113(8):2164–2169.

Cortesi, F. and Cheney, K. L. (2010). Conspicuousness is correlated with toxicity in marine opisthobranchs. Journal of Evolutionary Biology, 23(7):1509–1518.

Dalziell, A. H. and Welbergen, J. A. (2016). Mimicry for all modalities. Ecology Letters, 19(6):609–619.

Darragh, K., Vanjari, S., Mann, F., Gonzalez-Rojas, M. F., Morrison, C. R., Salazar, C., Pardo-Diaz, C., Merrill, R. M., McMillan, W. O., Schulz, S., and Jiggins, C. D. (2017). Male sex pheromone components in *Heliconius* butterflies released by the androconia affect female choice. PeerJ, 5:e3953.

Devries, P., LANDE, R., and Murray, D. (1999). Associations of co–mimetic ithomiine butterflies on small spatial and temporal scales in a neotropical rainforest. Biological Journal of the Linnean Society, 67:73 – 85.

Elias, M., Gompert, Z., Jiggins, C., and Willmott, K. (2008). Mutualistic interactions drive ecological niche convergence in a diverse butterfly community. PLOS Biology, 6(12):1–1.

Estrada, C. and Jiggins, C. (2002). Patterns of pollen feeding and habitat preference among heliconius species. Ecological Entomology, 27:448 – 456.

Estrada, C. and Jiggins, C. D. (2008). Interspecific sexual attraction because of convergence in warning colouration: is there a conflict between natural and sexual selection in mimetic species? Journal of Evolutionary Biology, 21(3):749–760.

Flanagan, N. S., Tobler, A., Davison, A., Pybus, O. G., Kapan, D. D., Planas, S., Linares, M., Heckel, D., and McMillan, W. O. (2004). Historical demography of müllerian mimicry in the neotropical heliconius butterflies. Proceedings of the National Academy of Sciences, 101(26):9704–9709.

Franks, D. W. and Noble, J. (2004). Batesian mimics influence mimicry ring evolution. Proceedings of the Royal Society of London. Series B: Biological Sciences, 271(1535):191–196.

Franks, D. W., Ruxton, G. D., and Sherratt, T. N. (2009). Warning signals evolve to disengage batesian mimics. Evolution, 63(1):256–267.

Franks, D. W. and Sherratt, T. N. (2007). The evolution of multicomponent mimicry. Journal of Theoretical Biology, 244(4):631 – 639.

González-Rojas, M. F., Darragh, K., Robles, J., Linares, M., Schulz, S., McMillan, W. O., Jiggins, C. D., Pardo-Diaz, C., and Salazar, C. (2020). Chemical signals act as the main reproductive barrier between sister and mimetic heliconius butterflies. Proceedings of the Royal Society B: Biological Sciences, 287(1926):20200587.

Goodale, E. and Kotagama, S. W. (2006). Vocal mimicry by a passerine bird attracts other species involved in mixed-species flocks. Animal Behaviour, 72(2):471 – 477.

Grill, C. P. and Moore, A. (1998). Effects of a larval antipredator response and larval diet on adult phenotype in an aposematic ladybird beetle. Oecologia, 114:274–282.

Gröning, J. and Hochkirch, A. (2008). Reproductive interference between animal species. The Quarterly Review of Biology, 83(3):257–282. PMID: 18792662.

Hines, H. M., Counterman, B. A., Papa, R., Albuquerque de Moura, P., Cardoso, M. Z., Linares, M., Mallet, J., Reed, R. D., Jiggins, C. D., Kronforst, M. R., and McMillan, W. O. (2011). Wing patterning gene redefines the mimetic history of heliconius butterflies. Proceedings of the National Academy of Sciences, 108(49):19666–19671.

Iwasa, Y., Pomiankowski, A., and Nee, S. (1991). The evolution of costly mate preferences ii. the "handicap" principle. Evolution, 45(6):1431–1442.

Jiggins, C. D., Naisbit, R. E., Coe, R. L., and Mallet, J. (2001). Reproductive isolation caused by colour pattern mimicry. Nature, 411(6835):302–305.

Joron, M. and Iwasa, Y. (2005). The evolution of a müllerian mimic in a spatially distributed community. Journal of Theoretical Biology, 237(1):87 – 103.

Joron, M., Jiggins, C. D., Papanicolaou, A., and McMillan, W. O. (2006). Heliconius wing patterns: an evo-devo model for understanding phenotypic diversity. Heredity, 97(3):157–167.

Joshi, J., Prakash, A., and Kunte, K. (2017). Evolutionary assembly of communities in butterfly mimicry rings. The American Naturalist, 189(4):E58–E76.

Kapan, D. D. (2001). Three-butterfly system provides a field test of müllerian mimicry. Nature, 409(6818):338–340.

Kirkpatrick, M., Johnson, T., and Barton, N. (2002). General models of multilocus evolution. Genetics, 161(4):1727–1750.

Kronforst, M. R., Young, L. G., Kapan, D. D., McNeely, C., O'Neill, R. J., and Gilbert, L. E. (2006). Linkage of butterfly mate preference and wing color preference cue at the genomic location of wingless. Proceedings of the National Academy of Sciences, 103(17):6575–6580.

Kyogoku, D. (2015). Reproductive interference: ecological and evolutionary consequences of interspecific promiscuity. Population Ecology, 57(2):253–260.

Le Roy, C., Roux, C., Authier, E., Bastide, H., Debat, V., and Llaurens, V. (2020). Convergent morphology and divergent phenology: unravelling the coexistence of mimetic morpho butterfly species. bioRxiv.

Lev-Yadun, S. (2009). Müllerian mimicry in aposematic spiny plants. Plant Signaling & Behavior, 4(6):482–483. PMID: 19816137.

Llaurens, V., Billiard, S., and Joron, M. (2013). The effect of dominance on polymorphism in müllerian mimicry. Journal of Theoretical Biology, 337:101 – 110.

Llaurens, V., Joron, M., and Théry, M. (2014). Cryptic differences in colour among müllerian mimics: how can the visual capacities of predators and prey shape the evolution of wing colours? Journal of Evolutionary Biology, 27(3):531–540.

Llaurens, V., Le Poul, Y., Puissant, A., Blandin, P., and Debat, V. (2021). Convergence in sympatry: Evolution of blue-banded wing pattern in morpho butterflies. Journal of Evolutionary Biology, 34(2):284–295.

Mallet, J. and Barton, N. H. (1989). Strong natural selection in a warning-color hybrid zone. Evolution, 43(2):421–431.

Mallet, J. and Gilbert Jr., L. E. (1995). Why are there so many mimicry rings? correlations between habitat, behaviour and mimicry in heliconius butterflies. Biological Journal of the Linnean Society, 55(2):159–180.

Mallet, J. and Joron, M. (1999). Evolution of diversity in warning color and mimicry: Polymorphisms, shifting balance, and speciation. Annual Review of Ecology and Systematics, 30(1):201–233.

McPeek, M. A. and Gavrilets, S. (2006). The evolution of female mating preferences: Differentiation from species with promiscious males can promotes speciation. Evolution, 60(10):1967 – 1980.

Merrill, R. M., Chia, A., and Nadeau, N. J. (2014). Divergent warning patterns contribute to assortative mating between incipient heliconius species. Ecology and Evolution, 4(7):911–917.

Merrill, R. M., Neggazi, S., Morrison, C. R., Crisp, R., and McMillan, W. O. (2018). Experimental manipulation of heliconius warning patterns reduces harassment of previously mated females. bioRxiv.

Mérot, C., Frérot, B., Leppik, E., and Joron, M. (2015). Beyond magic traits: Multimodal mating cues in heliconius butterflies. Evolution, 69(11):2891–2904.

Nagylaki, T. (1993). The evolution of multilocus systems under weak selection. Genetics, 134(2):627–647.

Naisbit, R. E., Jiggins, C. D., and Mallet, J. (2001). Disruptive sexual selection against hybrids contributes to speciation between *Heliconius cydno* and *Heliconius melpomene*. Proceedings of the Royal Society of London. Series B: Biological Sciences, 268(1478):1849–1854.

Ojala, K., Lindsröm, L., and Mappes, J. (2007). Life-history constraints and warning signal expression in an arctiid moth. Functional Ecology, 21(6):1162–1167.

Pfennig, D. W. and Kikuchi, D. W. (2012). Competition and the evolution of imperfect mimicry. Current Zoology, 58(4):608–619.

Pomiankowski, A. and Iwasa, Y. (1993). Evolution of multiple sexual preferences by fisher's runaway process of sexual selection. Proceedings: Biological Sciences, 253(1337):173–181.

Rice, S. H. (2004). Evolutionary theory: mathematical and conceptual foundations. Sinauer Associates, Sunderland, Mass., USA.

Ruxton, G. D., Franks, D. W., Balogh, A. C. V., and Leimar, O. (2008). Evolutionary implications of the form of predator generalization for aposematic signals and mimicry in prey. Evolution, 62(11):2913–2921.

Sanders, K., Malhotra, A., and Thorpe, R. (2006). Evidence for a müllerian mimetic radiation in asian pitvipers. Proceedings of the Royal Society B: Biological Sciences, 273(1590):1135–1141.

Savage, J. M. and Slowinski, J. B. (1992). The colouration of the venomous coral snakes (family elapidae) and their mimics (families aniliidae and colubridae). Biological Journal of the Linnean Society, 45(3):235–254.

Schemske, D. W. (1981). Floral convergence and pollinator sharing in two bee-pollinated tropical herbs. Ecology, 62(4):946–954.

Sherratt, T. N. (2006). Spatial mosaic formation through frequency-dependent selection in müllerian mimicry complexes. Journal of Theoretical Biology, 240(2):165–174.

Sherratt, T. N. (2008). The evolution of müllerian mimicry. Die Naturwissenschaften, 95(8):681–695.

Springer, V. and Smith-Vaniz, W. (1972). Mimetic relationships involving fishes of the family blenniidae. Smithsonian Contributions Zoology, 112.

Symula, R., Schulte, R., and Summers, K. (2001). Molecular phylogenetic evidence for a mimetic radiation in peruvian poison frogs supports a müllerian mimicry hypothesis. Proceedings of the Royal Society of London. Series B: Biological Sciences, 268(1484):2415–2421.

Willmott, K. R., Robinson Willmott, J. C., Elias, M., and Jiggins, C. D. (2017). Maintaining mimicry diversity: optimal warning colour patterns differ among microhabitats in amazonian clearwing butterflies. Proceedings of the Royal Society B: Biological Sciences, 284(1855):20170744.

Yamaguchi, R. and Iwasa, Y. (2013). Reproductive character displacement by the evolution of female mate choice. Evolutionary Ecology Research, 15(1):25–41.

Appendix: The limits of evolutionary convergence in sympatry: reproductive interference and developmental constraints leading to local diversity in aposematic signals

1 Model 1: Evolution of mimicry toward a fixed community of defended species

In Section 1.1 we detail how some components of fitness can be approximated using that the genetic covariances of traits and preference are low. In Section 1.2 we detail the computation of the selection vector describing the impact of the selective forces an the evolution of traits and preference. In Section 1.3, in line with the weak selection hypothesis we suppose that the genetic correlation between trait and preference is at equilibrium and estimate this quantity. In Section 1.4 we compute the values of trait and preference that cancel the leading term of the selection vector. In Section 1.5 we study when trait and preference converge toward the point found in the previous section. In Section 1.6 we study the impact of weak or strong female choosiness hypothesis on the phenotypic distance between *focal* species and the *local mimicry ring*. In Section 1.7 we detail the impact of each parameter of the phenotypic distance between the *focal* species and the *local mimicry ring*.

1.1 Low variance approximation

Because we assume that the variance of traits and preference is low we may use approximations in Equations (10) and (13). Here we detail how we obtained these approximations. The reasoning is similar for each approximation so we only explain how we get an approximation of $\mathcal{D}$ in (10). We recall that $\mathcal{D}$ is defined by

$$\mathcal{D}(t) = \lambda N \int_{\tau} f(\tau) \exp\left[-b(t-\tau)^2\right] \mathrm{d}\tau + \lambda' N' \int_{t'} g(t') \exp\left[-b(t-t')^2\right] \mathrm{d}t'.$$

We first approximate the first term of $\mathcal{D}$. We have

$$\int_{\tau} f(\tau) \exp\left[-b(t-\tau)^2\right] \mathrm{d}\tau = \exp\left[-b(t-\bar{t})^2\right] \int_{\tau} f(\tau) \exp\left[b(2t-\tau-\bar{t})(\tau-\bar{t})\right] \mathrm{d}\tau.$$

Using a Taylor expansion of $\exp\left[b(2t-\tau-\bar{t})(\tau-\bar{t})\right]$ we have

$$\exp\left[-b(t-\bar{t})^2\right] \int_{\tau} f(\tau) \left(1 + b(2t-\tau-\bar{t})(\tau-\bar{t}) + O((\tau-\bar{t})^2)\right) \mathrm{d}\tau,$$

which is equal to

$$\exp\left[-b(t-\bar{t})^2\right] \left(1 - b\mathrm{Var}(t) + O(\mathrm{Var}(t))\right).$$

Hence when the variance of t is low the first term of $\mathcal{D}$ can be approximated by

$$\lambda N \exp\left[-b(t-\bar{t})^2\right].$$

Similar computations for the other term give the approximation in Equation (10).

1.2 Selection coefficients

In this section we detail how we obtain the expression for the selection vector.

1.2.1 Computation of β_t

For the sake of readability, we first recall the definitions of the quantities under study.

The selective forces acting on the trait value write:

$$\begin{aligned}
\beta_t &= \frac{\partial}{\partial t_m} \ln W(t_m, t_f, p_f) + \frac{\partial}{\partial t_f} \ln W(t_m, t_f, p_f)\Big|_{(t_m,t_f,p_f)=(\bar{t},\bar{t},\bar{p})} \\
&= \frac{\partial}{\partial t_m} \left\{-a(p_f - t_m)^2 + \ln W_{pred}(t_m) - s(t_m - t_a)^2\right\}\Big|_{(t_m,t_f,p_f)=(\bar{t},\bar{t},\bar{p})} \\
&\quad + \frac{\partial}{\partial t_f} \left\{\ln W_{pred}(t_f) - s(t_f - t_a)^2\right\}\Big|_{(t_m,t_f,p_f)=(\bar{t},\bar{t},\bar{p})} \\
&= -2a(\bar{t} - \bar{p}) + 2\,\frac{\partial}{\partial t} \ln\left(W_{pred}(t)\right)\Big|_{t=\bar{t}} - 4s(\bar{t} - t_a).
\end{aligned}$$

Recall the definition of W_{pred} in (11). The second term of the right hand side equals

$$\begin{aligned}
2\frac{\partial}{\partial t} \ln\left(W_{pred}(t)\right) = &-4b\left((t - \bar{t}')\bar{\lambda}' \exp\left[-b(t - \bar{t}')^2\right]N' + (t - \bar{t})\lambda \exp\left[-b(t - \bar{t})^2\right]N\right) \\
&\left(\frac{1}{1 + \lambda N \exp\left[-b(t - \bar{t})^2\right] + \bar{\lambda}' \exp\left[-b(t - \bar{t}')^2\right]N' - d}\right. \\
&\left. - \frac{1}{1 + \lambda N \exp\left[-b(t - \bar{t})^2\right] + \bar{\lambda}' \exp\left[-b(t - \bar{t}')^2\right]N'}\right).
\end{aligned}$$

When the parameters b and d are of order ε (under (H_w)), we obtain

$$\beta_t = -2a(\bar{t} - \bar{p}) - \frac{4bd(\bar{t} - \bar{t}')\bar{\lambda}' N'}{\left(1 + \lambda N + \bar{\lambda}' N'\right)^2} - 4s(\bar{t} - t_a) + O(\varepsilon^3). \tag{A1}$$

1.2.2 Computation of β_p

Here again we recall the expression of selective forces acting on the preference value:

$$\begin{aligned}
\beta_p &= \frac{\partial}{\partial p_f} \ln W(t_m, t_f, p_f)\Big|_{(t_m,t_f,p_f)=(\bar{t},\bar{t},\bar{p})} \\
&= \frac{\partial}{\partial p_f} \left\{-a(p_f - t_m)^2 + \ln W_{RI}(p_f)\right\}\Big|_{(t_m,t_f,p_f)=(\bar{t},\bar{t},\bar{p})}.
\end{aligned}$$

The last term of the right hand side equals

$$\begin{aligned}\frac{\partial}{\partial p_f}\ln\left(W_{RI}(p_f)\right) &= -\ln\left(1+c_{RI}\exp\left[a(\bar{t}-\bar{t}')(\bar{t}+\bar{t}'-2p)\right]\frac{N'}{N}\right)\\ &\quad -\frac{-2c_{RI}a(\bar{t}-\bar{t}')\exp\left[a(\bar{t}-\bar{t}')(\bar{t}+\bar{t}'-2p)\right]\frac{N'}{N}}{1+c_{RI}\exp\left[a(\bar{t}-\bar{t}')(\bar{t}+\bar{t}'-2p)\right]\frac{N'}{N}}\\ &= \frac{2c_{RI}a(\bar{t}-\bar{t}')}{c_{RI}+\exp\left[a(\bar{t}-\bar{t}')(2p-\bar{t}-\bar{t}')\right]\frac{N}{N'}}.\end{aligned}$$

When the parameters a and c_{RI} are of order ε (under (H_w)), we finally obtain

$$\beta_p = -2a(\overline{p}-\bar{t}) + 2c_{RI}a(\bar{t}-\bar{t}')\frac{N'}{N} + O(\varepsilon^3). \tag{A2}$$

1.3 Computation of the matrix of correlation

In this part we approximate the genetic covariance between trait and preference C_{tp}, using the results from [Kirkpatrick et al., 2002]. Trait and preference are controled by different sets of unlinked loci with additive effects, denoted T and P, respectively. For each i in T (resp. P), we note ξ_i^t (resp. ξ_i^p) the contribution of the locus i on trait (resp. preference) value. The trait and preference values of an individual are then given by

$$t = \sum_{i\in T}\xi_i^t \quad \text{and} \quad p = \sum_{i\in P}\xi_i^p. \tag{A3}$$

As in [Lande, 1981] we assume that the distributions of ξ_i^t and ξ_i^p are multivariate Gaussian. Let C_{ij} be the genetic covariance between loci i and j. Then the elements of the matrix of correlation are given by:

$$G_t = \sum_{i,j\in T} C_{ij}, \quad G_p = \sum_{i,j\in P} C_{ij} \quad \text{and} \quad C_{tp} = \sum_{i\in T, j\in P} C_{ij}. \tag{A4}$$

To compute the change on genetic correlation we need to identify various selection coefficients (see [Barton and Turelli, 1991, Kirkpatrick et al., 2002]). These coefficients are obtained using the fitness of a mated pair of a male with trait t_m and a female with trait t_f and preference p_f $W(t_m, t_f, p_f)$ defined in Equation (1).

For simplicity we consider only leading terms in the change in genetic correlation. For $(i, j) \in T \times P$, combining Equations (9), (12), (15) from Kirkpatrick et al. [2002] gives the change in the genetic covariance between loci i and j:

$$\begin{aligned}\Delta C_{ij} = &- \frac{C_{ij}}{2} + \frac{1}{4}\tilde{a}_{t_m t_m} \sum_{k,l \in T} (C_{ik}C_{jl} + C_{il}C_{jk}) + \frac{1}{4}\tilde{a}_{p_f p_f} \sum_{k,l \in P} (C_{ik}C_{jl} + C_{il}C_{jk}) \\ &+ \frac{1}{4}\tilde{a}_{t_m p_f} \sum_{k \in T, l \in P} C_{ik}C_{jl} + \frac{1}{4}\tilde{a}_{t_m p_f} \sum_{k \in T, l \in P} C_{il}C_{jlk} + O(\varepsilon^2) \end{aligned} \tag{A5}$$

with $\tilde{a}_{\mu\rho}$ for $(\mu, \rho) \in \{t_m, t_f, p_f\}^2$ being the leading term of

$$a_{\mu\rho} := \frac{1}{2} \frac{\partial^2}{\partial\mu\partial\rho} \ln(W(t_m, t_f, p_f))\Big|_{(t_m, t_f, p_f) = (\bar{t}, \bar{t}, \bar{p})},$$

the selection coefficient calculated from the fitness of a mated pair of a male with trait t_m and a female with trait t_f and preference p_f. The expressions of these coefficients are:

$$a_{p_f p_f} = - a - \frac{2c_{RI}a^2(\bar{t} - \bar{t}')^2 \frac{N}{N'} \exp\left[a(\bar{t} - \bar{t}')(2\bar{p} - \bar{t} - \bar{t}')\right]}{\left(c_{RI} + \frac{N}{N'} \exp\left[a(\bar{t} - \bar{t}')(2\bar{p} - \bar{t} - \bar{t}')\right]\right)^2},$$

$$
\begin{aligned}
a_{t_m t_m} = &- a - s + 2b^2 \left(\overline{\lambda}' N' \left(1 + (\bar{t} - \bar{t}')^2 \right) \exp\left[b(\bar{t} - \bar{t}')^2 \right] + \lambda N \right) \\
&\times \left(\frac{1}{1 + \lambda N + \overline{\lambda}' N' \exp\left[b(\bar{t} - \bar{t}')^2 \right] - d} - \frac{1}{1 + \lambda N + \overline{\lambda}' N' \exp\left[b(\bar{t} - \bar{t}')^2 \right]} \right) \\
&+ \left(2b\overline{\lambda}' N' (\bar{t} - \bar{t}') \exp\left[b(\bar{t} - \bar{t}')^2 \right] \right)^2 \\
&\times \left(\frac{1}{\left(1 + \lambda N + \overline{\lambda}' N' \exp\left[b(\bar{t} - \bar{t}')^2 \right] - d \right)^2} - \frac{1}{\left(1 + \lambda N + \overline{\lambda}' N' \exp\left[b(\bar{t} - \bar{t}')^2 \right] \right)^2} \right),
\end{aligned}
$$

and

$$
a_{t_m p_f} = 2a.
$$

A Taylor expansion gives $\tilde{a}_{p_f p_f} = -a$, $\tilde{a}_{t_m t_m} = -a$ and $\tilde{a}_{t_m p_f} = 2a$.

By summing Equations (A5) over each i, j in T and P we obtain:

$$
\Delta C_{tp} = - \frac{C_{tp}}{2} - \frac{1}{2} a G_t C_{tp} - \frac{1}{2} a G_p C_{tp} + \frac{1}{2} a G_t G_p + \frac{1}{2} a C_{tp}^2 + O(\varepsilon^2). \tag{A6}
$$

For the sake of simplicity we assumed that the genetic correlations between traits and preferences are at equilibrium (as in [Barton and Turelli, 1991, Pomiankowski and Iwasa, 1993]). We obtain from (A6) that the value at equilibrium is given by

$$
C_{tp}^* = \frac{1 + a(G_p + G_t) - \sqrt{-4a^2 G_p G_t + (1 + a(G_p + G_t))^2}}{2a}.
$$

Because the genetic variances of trait and preference are low we have

$$
C_{tp}^* \approx a G_t G_p.
$$

When we relax the hypothesis $a = O(\varepsilon)$ and $b = O(\varepsilon)$ the previous calculation still stands, except that $\tilde{a}_{p_f p_f}$, $\tilde{a}_{t_m t_m}$ and $\tilde{a}_{t_m p_f}$ are of order 1 instead of being of order ε.

1.4 Quasi equilibria

We search mean values of trait and preference at equilibrium $\overline{t}^*$ and $\overline{p}^*$ such as the leading terms of $\Delta\overline{t}$ and $\Delta\overline{p}$ are null. We remind that we assume weak female choosiness and predator discrimination (default hypothesis (H_w)). The leading terms of $\Delta\overline{t}^*$ and $\Delta\overline{p}^*$ are thus $\tilde{\beta}_t = \tilde{\beta}_p = 0$ with

$$\tilde{\beta}_t = -2a(\overline{t}^* - \overline{p}^*) - \frac{4bd(\overline{t}^* - \overline{t}')\overline{\lambda}' N'}{\left(1 + \lambda N + \overline{\lambda}' N'\right)^2} - 4s(\overline{t}^* - t_a), \tag{A7}$$

$$\tilde{\beta}_p = -2a(\overline{p}^* - \overline{t}^*) + 2c_{RI}a(\overline{t}^* - \overline{t}')\frac{N'}{N}. \tag{A8}$$

We call such points quasi equilibria because they are not equilibrium point of Equation (6) but only cancel the term of leading order.

Lemma 1. *If*

$$\frac{2bd\overline{\lambda}' N'}{(\lambda N + \overline{\lambda}' N' + 1)^2} + 2s - \frac{ac_{RI}N'}{N} \neq 0, \tag{A9}$$

there is one quasi equilibrium point $(\overline{t}^*, \overline{p}^*)$*, where*

$$\overline{t}^* = \frac{\frac{2bd\overline{\lambda}' N'}{(1+\lambda N+\overline{\lambda}' N')^2}\overline{t}' + 2st_a - \frac{ac_{RI}N'}{N}\overline{t}'}{\frac{2bd\overline{\lambda}' N'}{(1+\lambda N+\overline{\lambda}' N')^2} + 2s - \frac{ac_{RI}N'}{N}} \quad \textit{and} \quad \overline{p}^* = \overline{t}^* + c_{RI}(\overline{t}^* - \overline{t}')\frac{N'}{N}. \tag{A10}$$

Proof. Assume that $a \neq 0$. From the definitions of $\tilde{\beta}_t$ and $\tilde{\beta}_p$ in (A7) and (A8), we deduce that the values of trait and preference $(\overline{t}^*, \overline{p}^*)$ for which the selections on trait and preference are null satisfy:

$$\tilde{\beta}_t = 0 \iff a(\overline{p}^* - \overline{t}^*) = \frac{2bd(\overline{t}^* - \overline{t}')\overline{\lambda}' N'}{\left(1 + \lambda N + \overline{\lambda}' N'\right)^2} + 2s(\overline{t}^* - t_a), \tag{A11}$$

and

$$\tilde{\beta}_p = 0 \iff a(\overline{p}^* - \overline{t}^*) = ac_{RI}(\overline{t}^* - \overline{t}')\frac{N'}{N}. \tag{A12}$$

From (A11) and (A12) we derivate:

$$\frac{2bd(\overline{t}^* - \overline{t}')\overline{\lambda}'N'}{\left(1 + \lambda N + \overline{\lambda}'N'\right)^2} + 2s(\overline{t}^* - t_a) = ac_{RI}(\overline{t}^* - \overline{t}')\frac{N'}{N}.$$

By factorizing by $\overline{t}$ we get:

$$\overline{t}^*\left(\frac{2bd\overline{\lambda}'N'}{\left(1 + \lambda N + \overline{\lambda}'N'\right)^2} + 2s - ac_{RI}\frac{N'}{N}\right) = \overline{t}'\left(\frac{2bd\overline{\lambda}'N'}{\left(1 + \lambda N + \overline{\lambda}'N'\right)^2} - ac_{RI}\frac{N'}{N}\right) + 2st_a. \tag{A13}$$

Using (A9), we obtain the value of $\overline{t}^*$ given in (A10). From (A12) we deduce the associated mean preference and conclude the proof. □

1.5 Fast and slow dynamics.

In this section we study when trait and preference in the *focal* species converge towards the quasi equilibrium point.

We suppose that the parameters are such as $\frac{2bd\overline{\lambda}'N'}{(\lambda N+\overline{\lambda}'N'+1)^2} + 2s - \frac{ac_{RI}N'}{N}$ is not of an order inferior to ε^2. We may have two long term behaviours. In case of convergence (case 1. of Lemma 2), the trajectories quickly approach the line $\overline{t} = \overline{p}$, before evolving according to a slower dynamic along this line (see the proof of Lemma 2 and Figures 1 and 2).

Lemma 2. *1. If*

$$\frac{2bd\overline{\lambda}'N'}{(\lambda N + \overline{\lambda}'N' + 1)^2} + 2s - \frac{ac_{RI}N'}{N} > 0,$$

the quantities $(\bar{t}-\bar{t}^*)$ *and* $(\bar{p}-\bar{p}^*)$ *become of order* $\sqrt{\varepsilon}$ *when the number of generations goes to infinity, where the values of* $\bar{t}^*$ *and* $\bar{p}^*$ *have been given in* (A10).

2. *If*

$$\frac{2bd\overline{\lambda}'N'}{(\lambda N+\overline{\lambda}'N'+1)^2}+2s-\frac{ac_{RI}N'}{N}<0,$$

trait and preference become very large.

Proof. As we have said, we can then decompose the dynamics into two steps. In the first one the leading order terms of the selection coefficient are the terms describing sexual selection and cost of choosiness. In this case we can approximate $\Delta(\bar{t}-\bar{p})^2$.

$$\begin{aligned}
\Delta(\bar{t}-\bar{p})^2 &= (\bar{t}+\Delta\bar{t}-\bar{p}-\Delta\bar{p})^2-(\bar{t}-\bar{p})^2\\
&= 2(\bar{t}-\bar{p})(\Delta\bar{t}-\Delta\bar{p})+(\Delta\bar{t}-\Delta\bar{p})^2\\
&= 2(\bar{t}-\bar{p})(\frac{1}{2}G_t\beta_t-\frac{1}{2}G_p\beta_p)+(\frac{1}{2}G_t\beta_t-\frac{1}{2}G_p\beta_p)^2\\
&= -(\bar{t}-\bar{p})\Bigg(2a(G_t+G_p)(\bar{t}-\bar{p})-a^2(G_p+G_t)^2(\bar{t}-\bar{p})\\
&\quad -2\left(\frac{ac_{RI}G_pN'(\bar{t}'-\bar{t})}{N}+\frac{2bdG_t\overline{\lambda}'N'(\bar{t}'-\bar{t})}{(lN+\overline{\lambda}'N'+1)^2}+G_ts(t_a-\bar{t})\right)\Bigg)+O(\varepsilon^3),
\end{aligned}$$

where we used (6) for the third equality and (A1) and (A2) for the last one. As by assumption, a, c_{RI}, b and d are of order ε, and s of order ε^2, we obtain

$$\Delta(\bar{t}-\bar{p})^2=-(\bar{t}-\bar{p})\Big(2a(G_t+G_p)(\bar{t}-\bar{p})+O(\varepsilon^2)\Big)+O(\varepsilon^3). \tag{A14}$$

Denote by r_n the value of $(\bar{t}-\bar{p})^2$ at generation n. We will prove the following statement:

$$\text{There exists } \alpha>0 \text{ such that for } n \text{ large enough, } r_n\leq 2\alpha\varepsilon^2. \tag{A15}$$

If we introduce the parameter

$$\mathcal{A}:=1-2a(G_t+G_p),$$

Equation (A14) may be rewritten:

$$r_{n+1} = \mathcal{A} r_n + \sqrt{r_n} f_n(1,\varepsilon) + f_n(2,\varepsilon),$$

for every $n \in \mathbb{N}$ $|f_n(1,\varepsilon)| \leq c_1\varepsilon^2$, $|f_n(2,\varepsilon)| \leq c_2\varepsilon^3$ where c_1 and c_2 are finite constants. Now introduce the variable

$$\rho_n := r_n - r_0\mathcal{A}^n.$$

As a is of order ε, and G_t and G_p of order one, there exists a positive and finite constant $C_{\mathcal{A}}$ such that for ε small enough,

$$0 < \mathcal{A} < 1 - C_{\mathcal{A}}\varepsilon.$$

We will choose in the sequel a positive real number α satisfying

$$\sqrt{\frac{2}{\alpha}} c_1 + \frac{c_2}{\alpha} < C_{\mathcal{A}} \tag{A16}$$

and

$$\frac{c_1}{\sqrt{\alpha}} + \frac{\sqrt{\alpha} c_1 + c_2}{\alpha} < C_{\mathcal{A}}. \tag{A17}$$

As $0 < \mathcal{A} < 1$, we see that for n large enough, $r_0\mathcal{A}^n \leq \alpha\varepsilon^2$. Thus to prove (A15), it is enough to prove that for n large enough, $|\rho_n| \leq \alpha\varepsilon^2$. We obtain for ρ the recurrence equation

$$\rho_{n+1} = \mathcal{A}\rho_n + \sqrt{\rho_n + r_0\mathcal{A}^n} f_n(1,\varepsilon) + f_n(2,\varepsilon). \tag{A18}$$

Assume first that $|\rho_n| \leq \alpha\varepsilon^2$. In this case,

$$\begin{aligned} |\rho_{n+1}| &\leq \mathcal{A}\alpha\varepsilon^2 + \sqrt{2\alpha\varepsilon^2} c_1\varepsilon^2 + c_2\varepsilon^3 \\ &= \alpha\varepsilon^2 \left(\mathcal{A} + \sqrt{\frac{2}{\alpha}} c_1\varepsilon + \frac{c_2}{\alpha}\varepsilon \right) \leq \alpha\varepsilon^2 \end{aligned}$$

thanks to (A16) provided that ε is small enough. Hence it is enough to prove that there exists one n such that $\rho_n \leq \alpha\varepsilon^2$, and the inequality will hold for later generations.

Now assume that $\rho_n > \alpha\varepsilon^2$. Using that

$$\sqrt{\rho_n + r_0\mathcal{A}^n} \leq \sqrt{|\rho_n|} + \sqrt{r_0\mathcal{A}^n} \leq \sqrt{|\rho_n|} + \sqrt{\alpha}\varepsilon$$

for n large enough, we obtain from (A18)

$$\begin{aligned}
|\rho_{n+1}| &\leq \mathcal{A}|\rho_n| + \sqrt{|\rho_n|}c_1\varepsilon^2 + (\sqrt{\alpha}c_1 + c_2)\varepsilon^3 \\
&\leq \mathcal{A}|\rho_n| + \sqrt{|\rho_n|}c_1\sqrt{\frac{|\rho_n|}{\alpha}}\varepsilon + (\sqrt{\alpha}c_1 + c_2)\frac{|\rho_n|}{\alpha}\varepsilon \\
&= |\rho_n|\left(\mathcal{A} + \frac{c_1}{\sqrt{\alpha}}\varepsilon + \frac{\sqrt{\alpha}c_1 + c_2}{\alpha}\varepsilon\right).
\end{aligned}$$

Due to (A17), the term in bracket belongs to $(0,1)$ if ε is small enough. We conclude that there exists n_0 such that $|\rho_n| \leq \alpha\varepsilon^2$ for any $n \geq n_0$. This concludes the proof of (A15) and of the fast convergent phase.

We now want to prove that $\bar{t}$ becomes close to $\bar{t}^*$, and $\bar{p}$ to $\bar{p}^*$. To this aim, we look at the variation of

$$\frac{(\bar{t} - \bar{t}^*)^2}{G_t} + \frac{(\bar{p} - \bar{p}^*)^2}{G_p},$$

where the values of $\bar{t}^*$ and $\bar{p}^*$ are the ones defined in (A10). By definition,

$$\Delta\left(\frac{(\bar{t} - \bar{t}^*)^2}{G_t} + \frac{(\bar{p} - \bar{p}^*)^2}{G_p}\right) = \frac{2\Delta\bar{t}(\bar{t} - \bar{t}^*) + \left(\Delta\bar{t}\right)^2}{G_t} + \frac{2\Delta\bar{p}(\bar{p} - \bar{p}^*) + (\Delta\bar{p})^2}{G_p}.$$

When $\bar{t} - \bar{p}$ is of order ε, $\Delta\bar{t}$ and $\Delta\bar{p}$ are of order ε^2. We then neglect the terms proportional to $\left(\Delta\bar{t}\right)^2$ and $(\Delta\bar{p})^2$. This yields

$$\begin{aligned}
\Delta\left(\frac{(\bar{t} - \bar{t}^*)^2}{G_t} + \frac{(\bar{p} - \bar{p}^*)^2}{G_p}\right) =& \frac{2\Delta\bar{t}(\bar{t} - \bar{t}^*)}{G_t} + \frac{2\Delta\bar{p}(\bar{p} - \bar{p}^*)}{G_p} + O(\varepsilon^4) \\
=& \beta_t(\bar{t} - \bar{t}^*) + \beta_p(\bar{p} - \bar{p}^*) + O(\varepsilon^4),
\end{aligned}$$

where we used (6). Now notice that

$$\bar{t}-\bar{t}^* = \bar{t}-\bar{p}+\bar{p}-\bar{p}^*+\bar{p}^*-\bar{t}^* = \bar{p}-\bar{p}^*+O(\varepsilon) = \frac{\bar{t}-\bar{t}^*}{2}+\frac{\bar{p}-\bar{p}^*}{2}+O(\varepsilon), \tag{A19}$$

as $\bar{p}-\bar{t}$ is of order ε and $\bar{p}^*-\bar{t}^*$ of order ε. We can make the same computation for $\bar{p}-\bar{p}^*$. Adding that β_t and β_p are of order ε^2, we obtain:

$$\Delta\left(\frac{(\bar{t}-\bar{t}^*)^2}{G_t}+\frac{(\bar{p}-\bar{p}^*)^2}{G_p}\right) = (\beta_t+\beta_p)\frac{\bar{t}-\bar{t}^*}{2}+(\beta_t+\beta_p)\frac{\bar{p}-\bar{p}^*}{2}+O(\varepsilon^3). \tag{A20}$$

Using (A1) and (A2) and simplifying, we get:

$$\beta_t+\beta_p = -\frac{4bd(\bar{t}-\bar{t}')\bar{\lambda}'N'}{\left(1+\lambda N+\bar{\lambda}'N'\right)^2}-4s(\bar{t}-t_a)+2c_{RI}a(\bar{t}-\bar{t}')\frac{N'}{N}+O(\varepsilon^3).$$

By substracting $-\frac{4bd(\bar{t}^*-\bar{t}')\bar{\lambda}'N'}{\left(1+\lambda N+\bar{\lambda}'N'\right)^2}-2s(\bar{t}^*-t_a)+2c_{RI}a(\bar{t}^*-\bar{t}')\frac{N'}{N}$ which is equal to zero (because $\beta_t|_{(t,p)=(\bar{t}^*,\bar{p}^*)}=0$ and $\beta_p|_{(t,p)=(\bar{t}^*,\bar{p}^*)}=0$, we get:

$$\beta_t+\beta_p = -\left(\frac{2bd\bar{\lambda}'N'}{\left(1+\lambda N+\bar{\lambda}'N'\right)^2}+2s-ac_{RI}\frac{N'}{N}\right)2(\bar{t}-\bar{t}^*)+O(\varepsilon^3) \tag{A21}$$

$$= -\left(\frac{2bd\bar{\lambda}'N'}{\left(1+\lambda N+\bar{\lambda}'N'\right)^2}+2s-ac_{RI}\frac{N'}{N}\right)2(\bar{p}-\bar{p}^*)+O(\varepsilon^3), \tag{A22}$$

where we used (A19). Replacing $\beta_t+\beta_p$ using (A21) and (A22) into (A20) yield:

$$\Delta\left(\frac{(\bar{t}-\bar{t}^*)^2}{G_t}+\frac{(\bar{p}-\bar{p}^*)^2}{G_p}\right) = -A\left((\bar{t}-\bar{t}^*)^2+(\bar{p}-\bar{p}^*)^2\right)+O(\varepsilon^3), \tag{A23}$$

with

$$A := \left(\frac{2bd\bar{\lambda}'N'}{\left(1+\lambda N+\bar{\lambda}'N'\right)^2}+2s-ac_{RI}\frac{N'}{N}\right). \tag{A24}$$

First case: $A > 0$

We suppose that the parameters are such that A is not of an order inferior to ε^2. Using computations similar to the ones derived to prove (A15), we may prove that after a number of generations large enough, $(\bar{t} - \bar{t}^*)^2$ and $(\bar{p} - \bar{p}^*)^2$ become of order ε, and thus $\bar{t} - \bar{t}^*$ and $\bar{p} - \bar{p}^*$ become of order $\varepsilon^{1/2}$.

To illustrate this result we simulated two trajectories of the system (6) $((\bar{t}_n^1, \bar{p}_n^1))_{n\in\mathbb{N}}$ and $((\bar{t}_n^2, \bar{p}_n^2))_{n\in\mathbb{N}}$ for two different initial conditions: (t^{i1}, p^{i1}) and (t^{i2}, p^{i2}). The trajectories are shown in Figure 1 and the parameter values are given in the caption. The parameter values correspond to the weak selection hypothesis and are such that $A > 0$.

The fast and slow dynamics are visible in Figure 1(a) where the trajectories quickly become close to the line defined by $\bar{t} = \bar{p}$ and then slowly converge toward the quasi equilibrium points. We noted $(\bar{t}^{eq}, \bar{p}^{eq})$ the equilibrium point reached by the two simulated trajectories.

Second case: $A < 0$**.**

Recall (A23) and that we assumed that A is not of order inferior to ε^2. This entails that $(\bar{t} - \bar{t}^*)^2/G_t + (\bar{p} - \bar{p}^*)^2/G_p$ goes to infinity. However when $t - \bar{t}'$ or $p - \bar{p}'$ becomes high (for example of order $1/\varepsilon$) the approximation

$$\exp\left[a(t - \bar{t}')(2p - t - \bar{t}')\right] = a(t - \bar{t}')(2p - t - \bar{t}') + O(\varepsilon^2)$$

does not stand. Therefore from a certain number of generations the approximation does not correctly describe the evolution of trait and preference. We can only conclude that trait and preference become very large. This is illustrated by Figure 2 which shows a simulation of two trajectories when $A < 0$. □

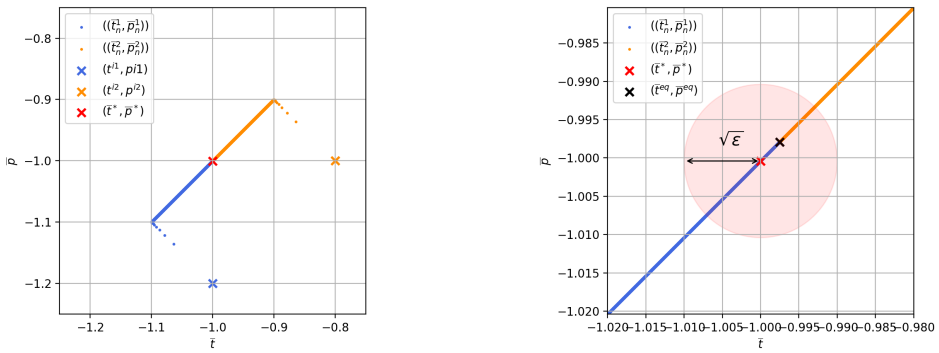

(a) (b)

Figure 1: (a) Evolution of mean trait value $\bar{t}$ and mean female preference value $\bar{p}$ for two different initial conditions. The blue (resp. orange) points represent the numerical trajectories for the initial condition (t^{i1}, p^{i1}) (resp. (t^{i2}, p^{i2})) (b) Zoom on the previous figure. The red circle has for center the quasi equilibrium point $(\bar{t}^*, \bar{p}^*)$ and for radius $\sqrt{\varepsilon}$. This illustrates that the numerical steady point $(\bar{t}^{eq}, \bar{p}^{eq})$ is at a distance of order $\sqrt{\varepsilon}$. The trajectories were obtained with the parameter values: $(t^{i1}, p^{i1}) = (-1, -1.2)$, $(t^{i2}, p^{i2}) = (-0.8, -1)$, a $= 10^{-4}$, b $= 2 \times 10^{-4}$, $d = 2 \times 10^{-4}$, $\lambda = 0.1$, $\bar{\lambda}' = 0.1$, $N = 10$, $N_p = 20$, $c_{RI} = 10^{-4}$, $s = 10^{-8}$, $\bar{t}' = 1$ and $t_a = 0$. The trajectories are computed over 1,000,000 generations.

1.6 Effect of weak or strong female choosiness on the phenotypic distances between the focal species and the local mimicry ring

Previously we obtained an analytic approximation of the phenotypic distance between the focal species and the local mimicry ring when the strengths of female choosiness (a) and predator discrimination (b) were weak (*i.e.* $a = O(\varepsilon)$ and $b = O(\varepsilon)$ (H_w)). To obtain this approximation we also assumed that the strength of developmental and selective constraints

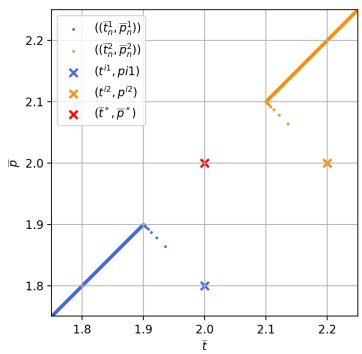

Figure 2: Evolution of mean trait value $\bar{t}$ and mean female preference value $\bar{p}$ for two different initial conditions. The blue (resp. orange) points represent the numerical trajectories for the initial condition (t^{i1}, p^{i1}) (resp. (t^{i2}, p^{i2})). The trajectories were obtained with the parameter values: $(t^{i1}, p^{i1}) = (-1, -1.2)$, $(t^{i2}, p^{i2}) = (-0.8, -1)$, a $= 10^{-4}$, b $= 2 \times 10^{-4}$, $d = 2 \times 10^{-4}$, $\lambda = 0.1$, $\overline{\lambda}' = 0.1$, $N = 10$, $N_p = 20$, $c_{RI} = 10^{-4}$, $s = 0.25 \times 10^{-8}$, $\bar{t}' = 1$ and $t_a = 0$. The trajectories are computed over 1,000,000 generations.

has the same order of magnitude as selection coefficients due to predation and reproductive interference (*i.e.* $s = O(\varepsilon^2)$). Under this assumption, the phenotypic distance between the focal species and the local mimicry ring becomes very large (see Figure 3) when

$$c_{RI} \geq \frac{2N}{aN'} \left(\frac{bd\overline{\lambda}' N'}{(1 + \lambda N + \overline{\lambda}' N')^2} + s \right). \tag{A25}$$

As explained in the main manuscript, this unrealistic divergence (under the weak choosiness hypothesis ($a = O(\varepsilon)$)) suggests that reproductive interference promotes strong phenotype divergence between the focal species and the local mimicry ring. Under weak choosiness, only a large distance between females preference and the trait displayed by the

local mimicry ring leads to a reduction of fitness cost generated by RI. Because females preference generates sexual selection on males trait, the phenotype divergence between the focal species and the local mimicry ring becomes high. When we relax the weak choosiness hypothesis (H_s) and use numerical simulations, then a great cost of reproductive interference provokes large but still of order 1 phenotypic distance between the focal species and the local mimicry ring (see Figure 3). However, we observe that the lower female choosiness, the higher is phenotypic distance when the cost of reproductive interference increases. As explained above, when females are not very choosy, reproductive interference favors the evolution of larger phenotypic distances limiting heterospecific mating.

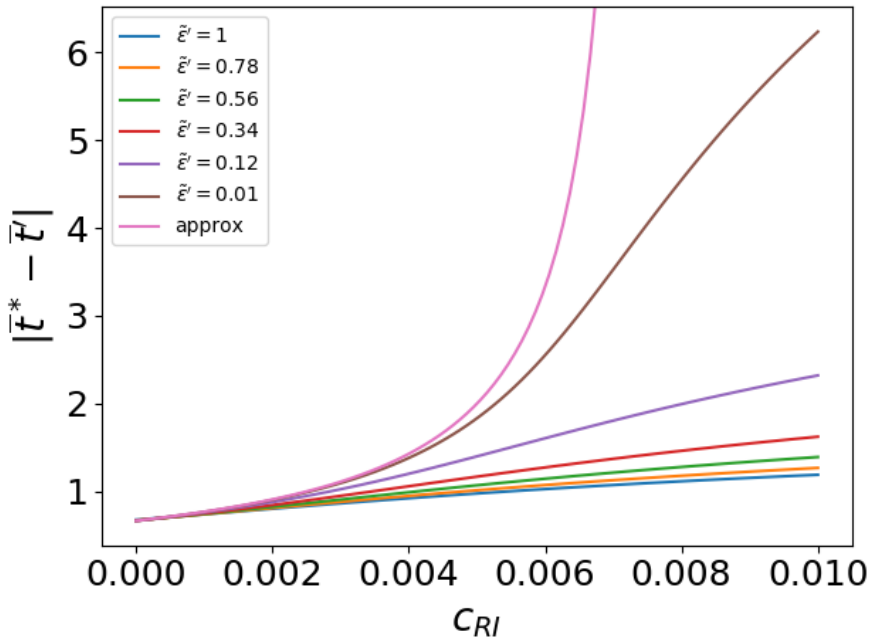

Figure 3: **Influence of the cost generated by reproductive interference c_{RI} on the phenotypic distances between the focal species and the local mimicry rings, using the analytical approximation ('approx' curve) or numerical simulations.** Different values of female choosiness (a), predator discrimination coefficient (b) and strength of selective and developmental constraints (s) are assumed for numerical simulations. This illustrate that curves obtained by numerical simulations tend to look similar to those using the analytical approximation where parameters values tends to satisfies (H_w). We assume: $a = \tilde{\varepsilon}'$, $b = \tilde{\varepsilon}'$, $s = 0.5\tilde{\varepsilon}\tilde{\varepsilon}'$,$d = 2\tilde{\varepsilon}$, $\lambda = 0.1$, $\overline{\lambda}' = 0.1$, $N = 10$, $N' = 20$, $t_a = 0$, $\bar{t}' = 1$.

1.7 Effect of different parameters on the level of trait divergence $|\bar{t}^* - \bar{t}'|$

We then aim at disentangling the effects of the different parameters of the model on trait divergence. We thus focus on the case where $A > 0$ (recall definition (A24)). In this case,

assuming weak female choosiness and predator discrimination (H_w), we know that the phenotypic distance between the focal species and the local mimicry ring, $|\bar{t}^* - \bar{t}'|$, equals

$$|\bar{t}^* - \bar{t}'| = \frac{2s|t_a - \bar{t}'|}{\frac{2bd\bar{\lambda}'N'}{(1+\lambda N+\bar{\lambda}'N')^2} + 2s - ac_{RI}\frac{N'}{N}},$$

allowing to investigate the relative impact of the different parameters on trait divergence. We also run numerical simulations to investigate the effect of the different parameters assuming strong females preference and predator discrimination (*i.e.* $a = O(1)$ and $b = O(1)$ (H_s)).

1.7.1 Effect of reproductive interference

Assuming weak female choosiness and predator discrimination (H_w), the impact of the strength of reproductive interference on the phenotypic distance between the focal species and the local mimicry ring is given by the sign of $\partial|\bar{t}^* - \bar{t}'|/\partial c_{RI}$. In our case,

$$\frac{\partial|\bar{t}^* - \bar{t}'|}{\partial c_{RI}} = \frac{2sa\frac{N'}{N}|t_a - \bar{t}'|}{\left(\frac{2bd\bar{\lambda}'N'}{(1+\lambda N+\bar{\lambda}'N')^2} + 2s - ac_{RI}\frac{N'}{N}\right)^2} > 0.$$

Hence the level of divergence increases with the strength of RI. A similar effect is observed assuming strong female choosiness and predator discrimination (H_s) (see Figure 4(a)). Similarly, assuming weak female choosiness and predator discrimination (H_w)

$$\frac{\partial|\bar{t}^* - \bar{t}'|}{\partial a} = \frac{2sc_{RI}\frac{N'}{N}|t_a - \bar{t}'|}{\left(\frac{2bd\bar{\lambda}'N'}{(1+\lambda N+\bar{\lambda}'N')^2} + 2s - ac_{RI}\frac{N'}{N}\right)^2} > 0,$$

thus the phenotypic distance (along with the strength of selection due to RI) increases with the strength of female choosiness. However, when female choosiness is strong and exceeds a threshold, females are able to distinguish males from their own species from individuals from the local mimicry rings, which limits divergence of the trait in the focal species (see

Figure 4(b)). Accurate female choice allows a quasi-similarity of the traits of the focal species and of the local mimicry ring, without implying heterospecific mating, relaxing the divergent selection exerted by RI.

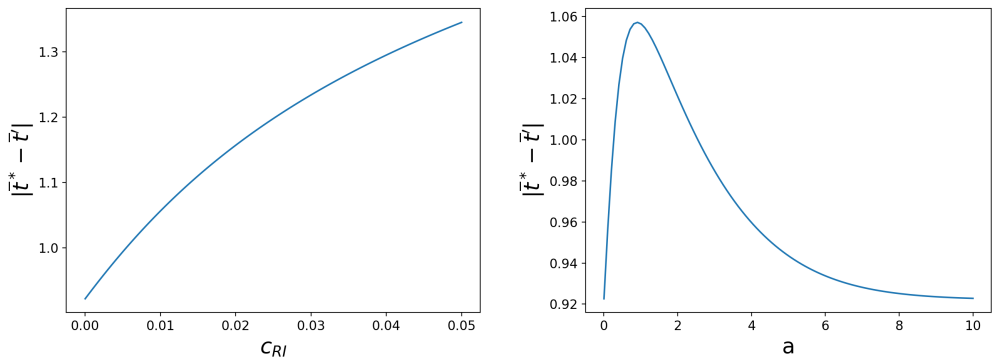

(a) (b)

Figure 4: **Influence of the strength of (a) reproductive interference c_{RI} and of (b) female choosiness a on the phenotypic distances between the focal species and the local mimicry rings, assuming strong female choosiness and predator discrimination.** The default parameters values are as follows: $a = 1$, $c_{RI} = 0.01$, $b = 1$, $d = 0.02$, $\lambda = 0.1$, $\overline{\lambda}' = 0.1$, $N = 10$, $N' = 20$, $s = 0.0025$, $t_a = 0$, $\bar{t}' = 1$.

1.7.2 Effect of predation

When a and b are of order ε (H_w),

$$\frac{\partial|\bar{t}^* - \bar{t}'|}{\partial d} = \frac{-2b\overline{\lambda}'N'}{(1+\lambda N+\overline{\lambda}'N')^2}\frac{2s|t_a - \bar{t}'|}{\left(\frac{2bd\overline{\lambda}'N'}{(1+\lambda N+\overline{\lambda}'N')^2} + 2s - ac_{RI}\frac{N'}{N}\right)^2} < 0,$$

hence the phenotypic distance decreases with the basal predation rate d. Assuming strong female choosiness and predator discrimination (H_s) leads to similar effect (Figure 5(a)).

When a and b are of order ε (H_w),

$$\frac{\partial|\bar{t}^* - \bar{t}'|}{\partial b} = \frac{-2d\overline{\lambda}'N'}{(1+\lambda N+\overline{\lambda}'N')^2} \frac{2s|t_a - \bar{t}'|}{\left(\frac{2bd\overline{\lambda}'N'}{(1+\lambda N+\overline{\lambda}'N')^2} + 2s - ac_{RI}\frac{N'}{N}\right)^2} < 0.$$

An increase on predator discriminating ability b thus also promotes phenotypic convergence as it increases the positive selection on mimicry generated by predation. Surprisingly, when a and b are of order 1 and predator discrimination exceeds a certain threshold, increased discrimination no longer promotes accurate mimicry (Figure 5(b)). When b is high, individuals from the focal species benefit from protection gained by mimicry only when they look very similar to the individuals of the local mimicry ring. Reproductive interference makes such high similarity too costly, and therefore divergence of the trait in the focal species becomes promoted (Figure 5(b)).

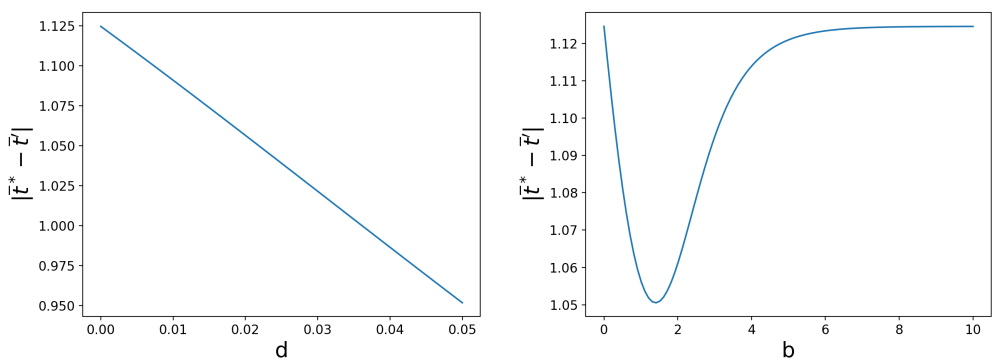

(a) (b)

Figure 5: **Influence of the strength of predation d (a) and of predator discrimination b (b) on the phenotypic distances between the focal species and the local mimicry rings, assuming strong female choosiness and predator discrimination.** The default parameters values are as follows: $a = 1$, $c_{RI} = 0.01$, $b = 1$, $d = 0.02$, $\lambda = 0.1$, $\overline{\lambda}' = 0.1$, $N = 10$, $N' = 20$, $s = 0.0025$, $t_a = 0$, $\bar{t}' = 1$.

1.7.3 Effect of the defence level of the focal species

Without reproductive interference ($c_{RI} = 0$) and when a and b are of order ε (H_w), we have

$$\frac{\partial|\bar{t}^* - \bar{t}'|}{\partial \lambda N} = \frac{2s|t_a - \bar{t}'|}{\left(\frac{2bd\overline{\lambda}' N'}{(1+\lambda N+\overline{\lambda}' N')^2} + 2s\right)} \frac{4bd\overline{\lambda}' N'}{(1+\lambda N+\overline{\lambda}' N')^3} > 0.$$

Therefore, the more defended the focal species is, the greater is the phenotypic distance between the focal species and the local mimicry ring.

Assuming reproductive interference generates cost ($c_{RI} > 0$), the density of the focal species then modulates the fitness cost incurred by RI. Therefore, we study the effect of the two components of the level of defence of the focal species: the individual defence level λ and the density N.

$$\frac{\partial|\bar{t}^* - \bar{t}'|}{\partial \lambda} = \frac{2bd\overline{\lambda}' N' N}{(1+\lambda N+\overline{\lambda}' N')^3} \frac{2s|t_a - \bar{t}'|}{\left(\frac{2bd\overline{\lambda}' N'}{(1+\lambda N+\overline{\lambda}' N')^2} + 2s - ac_{RI}\frac{N'}{N}\right)^2} > 0,$$

indicates that the individual defence level increases the phenotypic distance. Assuming strong female choosiness and predator discrimination leads to similar effect (Figure 6).

We also have

$$\frac{\partial|\bar{t}^* - \bar{t}'|}{\partial N} = -\frac{1}{N}\left(ac_{RI}\frac{N'}{N} - \frac{4bd(\lambda N)(\overline{\lambda}' N')}{(1+\lambda N+\overline{\lambda}' N')^3}\right) \frac{2s|t_a - \bar{t}'|}{\left(\frac{2bd\overline{\lambda}' N'}{(1+\lambda N+\overline{\lambda}' N')^2} + 2s - ac_{RI}\frac{N'}{N}\right)^2}.$$

While strong divergence is promoted when the focal species has a low abundance, for larger abundances, the effect of the density on the phenotypic distance between the focal species and the mimicry ring depends on the strength of reproductive interference and predation (Figure 7). When fitness cost due to reproductive interference is great compared to fitness cost due to predation, an increase in the density of the focal species decreases the phenotypic distance, because its reduces the fitness cost due to reproductive interference

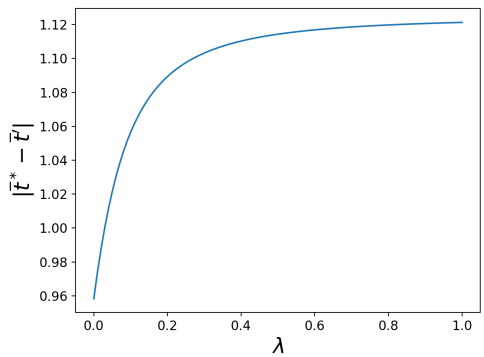

Figure 6: **Influence of the individual defence level λ on the phenotypic distances between the focal species and the local mimicry rings, assuming strong female choosiness and predator discrimination.** The default parameters values are as follows: $a = 1$, $c_{RI} = 0.01$, $b = 1$, $d = 0.02$, $\lambda = 0.1$, $\overline{\lambda}' = 0.1$, $N = 10$, $N' = 20$, $s = 0.0025$, $t_a = 0$, $\bar{t}' = 1$.

(similar effect observed assuming strong female choosiness and predator discrimination (H_s) (Figure 7(a))). By contrast, when fitness cost due to reproductive interference is low compared to fitness cost due to predation, an increase in the density of the focal species increases the phenotypic distance because the focal species is better defended (similar effect observed assuming strong female choosiness and predator discrimination (H_s) (see right part of Figure 7(b))).

1.7.4 Effect of selective and developmental constraints promoting the ancestral trait value t_a.

When a and b are of order ε,

$$\frac{\partial|\bar{t}^* - \bar{t}'|}{\partial s} = \frac{2|t_a - \bar{t}'|\left(\frac{2bd\overline{\lambda}'N'}{(1+\lambda N+\overline{\lambda}'N')^2} - ac_{RI}\frac{N'}{N}\right)}{\left(\frac{2bd\overline{\lambda}'N'}{(1+\lambda N+\overline{\lambda}'N')^2} + 2s - ac_{RI}\frac{N'}{N}\right)^2}.$$

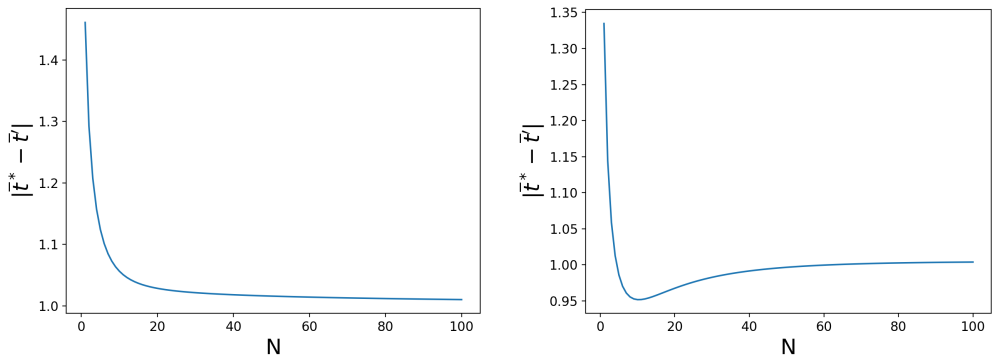

(a) (b)

Figure 7: **Influence of the density of the focal species N on the phenotypic distances between the focal species and the local mimicry rings, when (b) predation is low compared to reproductive interference and (b) when predation is high compared to RI, assuming strong female choosiness and predator discrimination.** Simulations were run assuming: (a) $d = 0.02$ or (b) $d = 0.05$. The default parameters values are as follows: $a = 1$, $c_{RI} = 0.01$, $b = 1$, $\lambda = 0.1$, $\overline{\lambda}' = 0.1$, $N = 10$, $N' = 20$, $s = 0.0025$, $t_a = 0$, $\bar{t}' = 1$.

Thus when selection due to predation is stronger than selection due to reproductive interference (i.e. $\frac{2bd\overline{\lambda}'N'}{(1+\lambda N+\overline{\lambda}'N')^2} > ac_{RI}\frac{N'}{N}$), selective and developmental constraints promotes the divergence of trait between the focal species and the local mimicry ring (similar effect observed assuming strong female choosiness and predator discrimination (Figure 8(b))). By contrast, when the selection due to reproductive interference is stronger than selection due to predation (i.e. $ac_{RI}\frac{N'}{N} > \frac{2bd\overline{\lambda}'N'}{(1+\lambda N+\overline{\lambda}'N')^2}$), selective and developmental constraints limits the trait divergence due to reproductive interference (similar effect observed assuming strong female choosiness and predator discrimination (Figure 8(a))).

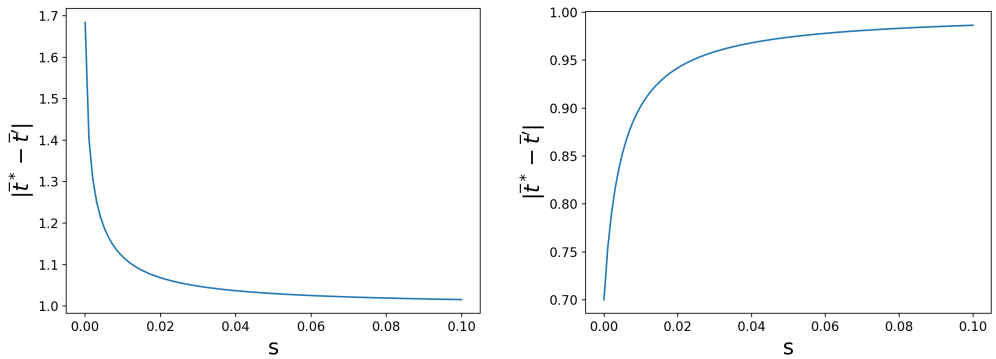

(a) (b)

Figure 8: **Influence of the strength of selective constraints s on the phenotypic distances between the focal species and the local mimicry rings, when (b) predation is low compared to reproductive interference and (b) when predation is great compared to RI, assuming strong female choosiness and predator discrimination.** Simulations were run assuming: (a) $d = 0.02$ or (b) $d = 0.05$. The default parameters values are as follows: $a = 1$, $c_{RI} = 0.01$, $b = 1$, $\lambda = 0.1$, $\overline{\lambda}' = 0.1$, $N = 10$, $N' = 20$, $s = 0.0025$, $t_a = 0$, $\bar{t}' = 1$.

1.7.5 Effect of the mimetic community.

Finally, we investigate the impact of the composition of the local mimicry ring (density N' and defense level λ') on trait divergence. When a and b are of order ε (H_w), we have:

$$\frac{\partial|\bar{t}^* - \bar{t}'|}{\partial\overline{\lambda}'} = \frac{2bdN'(\overline{\lambda}'N' - 1 - \lambda N)}{(1 + \lambda N + \overline{\lambda}'N')^3} \frac{2s|t_a - \bar{t}'|}{\left(\frac{2bd\overline{\lambda}'N'}{(1+\lambda N+\overline{\lambda}'N')^2} + 2s - ac_{RI}\frac{N'}{N}\right)^2},$$

and

$$\frac{\partial|\bar{t}^* - \bar{t}'|}{\partial N'} = \left(\frac{2bd\overline{\lambda}'(\overline{\lambda}'N' - 1 - \lambda N)}{(1 + \lambda N + \overline{\lambda}'N')^3} + \frac{ac_{RI}}{N}\right) \frac{2s|t_a - \bar{t}'|}{\left(\frac{2bd\overline{\lambda}'N'}{(1+\lambda N+\overline{\lambda}'N')^2} + 2s - ac_{RI}\frac{N'}{N}\right)^2}.$$

Thus, when the defence level of the local mimicry ring ($\overline{\lambda}'N'$) is lower than the defence level of the focal species plus one ($\overline{\lambda}'N' < 1+\lambda N$), an increase in the defence level of individuals of the local mimicry ring promotes phenotypic similarity between the focal species and the local mimicry ring (similar effect observed assuming strong but moderate female choosiness and predator discrimination (H_s) (Figure 9(a))). Indeed, an increase of $\overline{\lambda}'N'$ increases the advantage of looking similar to individuals of the local mimicry ring. More surprisingly, when the defence level of the local mimicry ring is greater ($\overline{\lambda}'N' > 1+\lambda N$), the phenotypic distance increases with $\overline{\lambda}'N'$ (similar effect observed assuming strong but moderate female choosiness and predator discrimination (Figure 9(a))). Under weak ($b = O(\varepsilon)$) or strong but moderate (*e.g.* $b = 1$) predator discrimination, predators tend to generalize mimetic trait. Then individuals of the focal species gain at least a little protection from the local mimicry ring, even when displaying a imperfectly mimetic trait. When the level of protection of the mimicry ring is high, the fitness costs linked to predation is low compared to the reproductive interference and decreases with the defence level of individuals of the local mimicry ring. This decrease in selection pressure generated by predation decreases the phenotype similarity between the focal species and the local mimicry ring. When predator discrimination is strong and high (*e.g.* $b = 10$), there is no generalization of imperfect mimics by predators, this effect is no longer observed (see Figure 9(b)).

The density N' and the individual defence level of the local mimicry ring λ' have the same effect on the overall defence level of the local mimicry ring (function of the parameter $\overline{\lambda}'N'$), and therefore have a similar effect on the phenotypic distance. However, the density of the local mimicry ring N' also plays a role on the fitness costs generated by RI. When the strength of reproductive interference is high as compared to predation, the phenotypic distance increases with the density of the local mimicry ring (N'), because

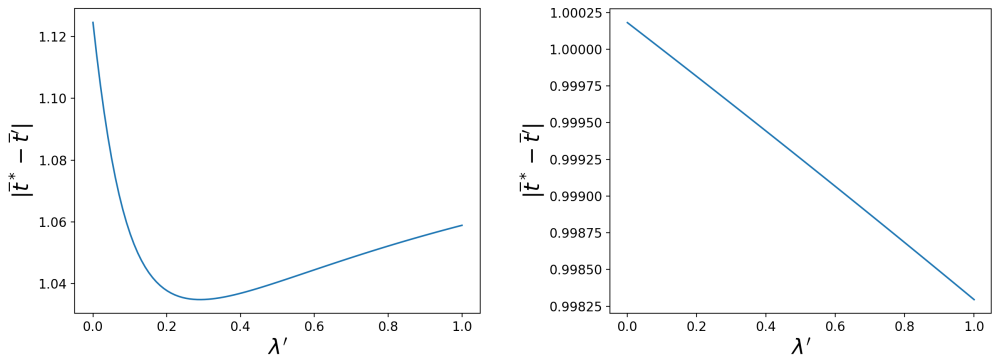

(a) (b)

Figure 9: **Influence of the mean defence level of individuals of the local mimicry ring $\overline{\lambda}'$ on the phenotypic distances between the focal species and the local mimicry rings for (a) moderate ($b = 1$) and (b) high ($b = 10$) predator discrimination, assuming strong female choosiness and predator discrimination (*i.e.* $a = O(1)$ and $b = O(1)$).** Simulations were run assuming: (a) $a = 1$ and (b) $a = 10$. The default parameters values are as follows: $a = 1$, $c_{RI} = 0.01$, $d = 0.02$, $\lambda = 0.1$, $\overline{\lambda}' = 0.1$, $N = 10$, $N' = 20$, $s = 0.0025$, $t_a = 0$, $\bar{t}' = 1$.

it increases the cost of reproductive interference (similar effect observed assuming strong female choosiness and predator discrimination (Figure 10(a))). When the strength of reproductive interference is low compared to predation, the density of the local mimicry ring (N') has a similar effect than the defence level of individuals of the local mimicry ring λ' on the phenotypic distance (similar effect observed assuming strong but moderate female choosiness and predator discrimination (Figure 10(b))).

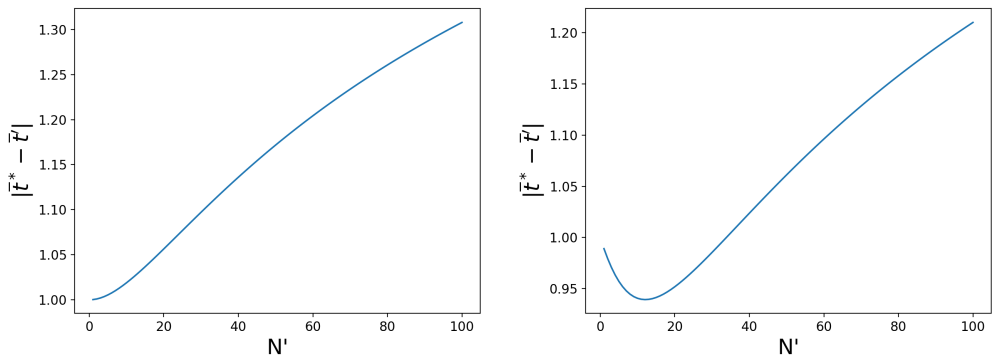

(a) (b)

Figure 10: **Influence of the density of the local mimicry ring N' on the phenotypic distances between the focal species and the local mimicry rings, when (b) predation is low compared to reproductive interference and (b) when predation is high compared to RI, assuming strong female choosiness and predator discrimination.** Simulations were run assuming: (a) $d = 0.02$ or (b) $d = 0.05$. The default parameters values are as follows: $a = 1$, $c_{RI} = 0.01$, $b = 1$, $\lambda = 0.1$, $\overline{\lambda}' = 0.1$, $N = 10$, $N' = 20$, $s = 0.0025$, $t_a = 0$, $\bar{t}' = 1$.

2 Model 2: Evolution of mimicry between two interacting species

In Section 2.1 we give the parameters used in the second model and their description. In Section 2.2 we detail the computations of the selection vectors in both species describing the impact of the selective forces an the evolution of trait and preference. In Section 2.3 we compute the values of trait and preference that cancel the leading term of the selection vectors in both species. In Section 2.4 we study when trait and preference converge toward the point found in the previous section. In Section 2.5 we detail the impact of each

Abbreviation	Description
$\bar{t}_i/\bar{p}_i$	Mean trait/preference value in the species i
G_{t_i}/G_{p_i}	Genetic variance of trait t_i/preference p_i
$C_{t_i p_i}$	Genetic covariance between trait t_i and preference p_i
β_{t_i}/β_{p_i}	Selection coefficient on trait t_i/preference p_i
a_i	Female choosiness in species i
s_i	Strength of developmental constraints in species i
t_{ai}	Ancestral trait favored by developmental constraints in species i
d	Basal predation rate
b	Predator discrimination
λ_i	Unpalatability coefficient of individuals of the species i
N_i	Density of the species i
c_{RI}	Strength of reproductive interference

Table 1: Description of variables and parameters used in the model with two species. The subscript $i \in \{1, 2\}$ denotes the species.

parameter of the interspecific phenotypic distance.

2.1 Parameters of the model

The parameters used in the model are summed up in Table 1 .

2.2 Selection coefficients

In this section we detail how we obtain the expressions for the selection vectors.

For $i \in \{1,2\}$, the selection coefficients are defined by:

$$\beta_{t_i} := \frac{\partial}{\partial t_m} \ln W^i(t_m, t_f, p_f) + \frac{\partial}{\partial t_f} \ln W^i(t_m, t_f, p_f)\Big|_{(t_m,t_f,p_f)=(\bar{t},\bar{t},\bar{p})},$$

$$\beta_{p_i} := \frac{\partial}{\partial p_f} \ln W^i(t_m, t_f, p_f)\Big|_{(t_m,t_f,p_f)=(\bar{t},\bar{t},\bar{p})},$$

where W^i are the fitness of a mated pair of a male with trait t_m and a female with trait t_f and preference p_f of the species i, and write

$$W^i(t_m, t_f, p_f) = W^i_{ns}(t_m) W^i_r(t_m, p_f) W^i_{ns}(t_f) W^i_{RI}(p_f).$$

Here W^i_{ns} is the impact of natural selection on fitness and W^i_{RI} is the impact reproductive interference on fitness of individuals of species i.

2.2.1 Computation of β_{t_1} and β_{t_2}

Similarly as the case of one population in a mimicry ring studied previously (recall the definition of W_{pred} in (11)), the impact of predation on an individual of trait t is:

$$\begin{aligned}\frac{\partial}{\partial t_1} \ln\left(W^2_{pred}(t_1)\right) = &-2b\Big((t_1-\bar{t}_1)\lambda_1 \exp\left[-b(t_1-\bar{t}_1)^2\right]N_1 + (t_2-\bar{t}_2)\overline{\lambda}_2 \exp\left[-b(t_2-\bar{t}_2)^2\right]N_2\Big)\\ &\times\Bigg(\frac{1}{1+\lambda_1 N_1 \exp\left[-b(t_2-\bar{t}_1)^2\right] + \lambda_2 \exp\left[-b(t_2-\bar{t}_2)^2\right]N_2 - d}\\ &-\frac{1}{1+\lambda_1 N_1 \exp\left[-b(t_2-\bar{t}_1)^2\right] + \lambda_2 \exp\left[-b(t_2-\bar{t}_2)^2\right]N_2}\Bigg).\end{aligned}$$

By symmetry we obtain the expression of $\frac{\partial}{\partial t_2} \ln\left(W^2_{pred}(t_2|\bar{t}_1,\bar{t}_2)\right)$ by exchanging 1 and 2. When b is of order ε (H_w), similar computations as in the case of one population in a mimicry ring yield:

$$\beta_{t_1} = -2a_1(\bar{t}_1 - \bar{p}_1) - \frac{4bd(\bar{t}_1-\bar{t}_2)\lambda_2 N_2}{(1+\lambda_1 N_1 + \lambda_2 N_2)^2} - 4s_1(\bar{t}_1 - t_{a1}) + O(\varepsilon^3), \tag{A26}$$

$$\beta_{t_2} = -2a_2(\bar{t}_2 - \bar{p}_2) - \frac{4bd(\bar{t}_2-\bar{t}_1)\lambda_1 N_1}{(1+\lambda_1 N_1 + \lambda_2 N_2)^2} - 4s_2(\bar{t}_2 - t_{a2}) + O(\varepsilon^3). \tag{A27}$$

2.2.2 Computation of β_{p_1} and β_{p_2}

Let $W^i_{RI}(p)$ indicate the impact of reproductive interference on a female of species i with preference p. If we denote by j the complement of i in $\{1,2\}$, we get:

$$W^i_{RI}(p_i) = \frac{\exp\left[-a_i(p_i-\bar{t}_i)^2\right]N_i}{\exp\left[-a_i(p_i-\bar{t}_i)^2\right]N_i + c_{RI}\exp\left[-a_j(p_i-\bar{t}_j)^2)\right]N_j}.$$

In the same way as in the previous model we thus get, when we assume that a_1, a_2 and c_{RI} are of order ε (H_w),

$$\beta_{p_1} = -2a_1(\overline{p}_1-\bar{t}_1) + 2c_{RI}a_1(\bar{t}_1-\bar{t}_2)\frac{N_2}{N_1} + O(\varepsilon^3), \tag{A28}$$

$$\beta_{p_2} = -2a_2(\overline{p}_2-\bar{t}_2) + 2c_{RI}a_2(\bar{t}_2-\bar{t}_1)\frac{N_1}{N_2} + O(\varepsilon^3). \tag{A29}$$

2.3 Quasi equilibria

We search mean values of traits and preferences at equilibrium $\bar{t}^*_1$, $\overline{p}^*_1$, $\bar{t}^*_2$ and $\overline{p}^*_2$ such as the leading terms of $\Delta\bar{t}^*_1$, $\Delta\overline{p}^*_1$, $\Delta\bar{t}^*_2$ and $\Delta\overline{p}^*_2$ are null, or equivalently, $\tilde{\beta}_{t_1} = \tilde{\beta}_{p_1} = \tilde{\beta}_{t_2} = \tilde{\beta}_{p_2} = 0$ with

$$\tilde{\beta}_{t_1} = -2a_1(\bar{t}^*_1-\overline{p}^*_1) - \frac{4bd(\bar{t}^*_1-\bar{t}^*_2)\lambda_2N_2}{(1+\lambda_1N_1+\lambda_2N_2)^2} - 4s_1(\bar{t}^*_1-t_{a1}), \tag{A30}$$

$$\tilde{\beta}_{p_1} = -2a_1(\overline{p}^*_1-\bar{t}^*_1) + 2c_{RI}a_1(\bar{t}^*_1-\bar{t}^*_2)\frac{N_2}{N_1}, \tag{A31}$$

$$\tilde{\beta}_{t_2} = -2a_2(\bar{t}^*_2-\overline{p}^*_2) - \frac{4bd(\bar{t}^*_2-\bar{t}^*_1)\lambda_1N_1}{(1+\lambda_1N_1+\lambda_2N_2)^2} - 4s_2(\bar{t}^*_2-t_{a2}), \tag{A32}$$

$$\tilde{\beta}_{p_2} = -2a_2(\overline{p}^*_2-\bar{t}^*_2) + 2c_{RI}a_2(\bar{t}^*_2-\bar{t}^*_1)\frac{N_1}{N_2}. \tag{A33}$$

Lemma 3. *Let us introduce for $i \neq j \in \{1,2\}^2$,*

$$A_i = \frac{2bd\lambda_jN_j - a_ic_{RI}\frac{N_j}{N_i}\left(1+\lambda_1N_1+\lambda_2N_2\right)^2}{2bd\lambda_jN_j + (2s_i - a_ic_{RI}\frac{N_j}{N_i})\left(1+\lambda_1N_1+\lambda_2N_2\right)^2}, \tag{A34}$$

$$B_i = \frac{2s_it_{ai}\left(1+\lambda_1N_1+\lambda_2N_2\right)^2}{2bd\lambda_jN_j + (2s_i - a_ic_{RI}\frac{N_j}{N_i})\left(1+\lambda_1N_1+\lambda_2N_2\right)^2}. \tag{A35}$$

If $2bd\lambda_j N_j + (2s_i - a_i c_{RI}(N_j/N_i))\,(1+\lambda_1 N_1 + \lambda_2 N_2)^2 \neq 0$ *for* $i \in \{1,2\}$ *and if* $A_1 A_2 \neq 1$ *there is a unique quasi equilibrium point given for* $i \in \{1,2\}$ *by*

$$\bar{t}_i^* = \frac{B_i + A_i B_j}{1 - A_1 A_2}, \quad \bar{p}_i^* = \bar{t}_i^* + c_{RI}(\bar{t}_i^* - \bar{t}_j^*)\frac{N_j}{N_i}, \tag{A36}$$

Remark. We do not give the quasi equilibrium traits and preferences when one of the following conditions is verified:

- $2bd\lambda_2 N_2 + (2s_1 - a_1 c_{RI}(N_2/N_1))\,(1+\lambda_1 N_1 + \lambda_2 N_2)^2 = 0,$
- $2bd\lambda_1 N_1 + (2s_2 - a_2 c_{RI}(N_1/N_2))\,(1+\lambda_1 N_1 + \lambda_2 N_2)^2 = 0,$
- $A_1 A_2 = 1.$

Indeed investigating those cases leads to a long enumeration of subcases with different quasi equilibrium points, and those cases are negligible compared with all the possible combinations of parameters. We thus choose to not give this enumeration.

Proof. Let $2bd\lambda_j N_j + (2s_i - a_i c_{RI}(N_j/N_i))\,(1+\lambda_1 N_1 + \lambda_2 N_2)^2 \neq 0$ for $i \neq j \in \{1,2\}^2$. Using the results of the first model (see Appendix 1.3) we have

$$\bar{t}_1^* = \frac{\frac{2bd\lambda_2 N_2}{(1+\lambda_1 N_1+\lambda_2 N_2)^2}\bar{t}_2^* + 2s_1 t_{a1} - a_1 c_{RI}\frac{N2}{N1}\bar{t}_2^*}{\frac{2bd\lambda_2 N_2}{(1+\lambda_1 N_1+\lambda_2 N_2)^2} + 2s_1 - a_1 c_{RI}\frac{N_2}{N_1}},$$

and

$$\bar{t}_2^* = \frac{\frac{2bd\lambda_1 N_1}{(1+\lambda_1 N_1+\lambda_2 N_2)^2}\bar{t}_1^* + 2s_2 t_{a2} - a_2 c_{RI}\frac{N1}{N2}\bar{t}_1^*}{\frac{2bd\lambda_1 N_1}{(1+\lambda_1 N_1+\lambda_2 N_2)^2} + 2s_2 - a_2 c_{RI}\frac{N_1}{N_2}},$$

which can be rewritten

$$\bar{t}_1^* = A_1\bar{t}_2^* + B_1, \quad \bar{t}_2^* = A_2\bar{t}_1^* + B_2,$$

where $(A_i, B_i), i \in \{1,2\}$ have been defined in (A34)-(A35).

If $A_1A_2 \neq 1$ there are unique values for traits at quasi equilibrium given by $\overline{t}_1^*$ and $\overline{t}_2^*$ defined in (A36). Using previous results we have the associated mean preferences at quasi equilibrium $\overline{p}_1^*$ and $\overline{p}_2^*$ defined in (A36).

□

2.4 Fast and slow dynamics.

In this section we study when trait and preference in the both species converge towards the quasi equilibrium point.

Lemma 4. *Let us introduce*

$$B_{pred} = \frac{2bd}{(1+\lambda_1 N_1 + \lambda_2 N_2)^2},$$
$$C_1 = 2\lambda_2 N_2 B_{pred} + 4s_1 - 2c_{RI}a_1\frac{N_2}{N_1},$$
$$C_2 = 2\lambda_1 N_1 B_{pred} + 4s_2 - 2c_{RI}a_2\frac{N_1}{N_2},$$

and recall the definitions of A_1 and A_2 in (A34).

1. *If $C_1 > 0$, $C_2 > 0$ and $C_1C_2(1-A_1A_2) - \frac{1}{4}(A_1C_1 - A_2C_2)^2 > 0$ the quantities $\overline{t}_1 - \overline{t}_1^*$, $\overline{t}_2 - \overline{t}_2^*$, $\overline{p}_1 - \overline{p}_1^*$ and $\overline{p}_2 - \overline{p}_2^*$ become of order $\sqrt{\varepsilon}$ when the number of generation goes to infinity, with $\overline{t}_1^*$, $\overline{t}_2^*$, $\overline{p}_1^*$ and $\overline{p}_2^*$ defined by (A36).*

2. *If $C_1 < 0$, $C_2 < 0$ and $C_1C_2(1-A_1A_2) - \frac{1}{4}(A_1C_1 - A_2C_2)^2 > 0$, traits and preferences become very large.*

Remark. When $C_1C_2(1-A_1A_2) - \frac{1}{4}(A_1C_1 - A_2C_2)^2 > 0$ or $C_1C_2 < 0$ we are not able to analytically determine the convergence or the divergence of traits and preferences. To infer such information we simulate the dynamic of traits and preferences considering the leading term of the selection coefficients.

Proof. As previously, we can decompose the dynamics into two steps. In the first one the leading order terms of the selection coefficient are the terms describing sexual selection and cost of choosiness. Using computations similar to the ones in the previous model we can approximate $\Delta(\bar{t}_i - \overline{p}_i)^2$ for $i \in \{1, 2\}$ by

$$\Delta(\bar{t}_i - \overline{p}_i)^2 = -(\bar{t}_i - \overline{p}_i)\Big(2a_i(G_{t_i} + G_{p_i})(\bar{t}_i - \overline{p}_i) + O(\varepsilon^2)\Big) + O(\varepsilon^3).$$

Using the same reasoning that in the previous model we may prove that above a certain number of generations $t_1 - p_1$ and $t_2 - p_2$ are of order ε.

We now look at the variation of

$$\mathcal{A} := \frac{(\bar{t}_1 - \bar{t}_1^*)^2}{G_{t_1}} + \frac{(\bar{t}_2 - \bar{t}_2^*)^2}{G_{t_2}} + \frac{(\overline{p}_1 - \overline{p}_1^*)^2}{G_{p_1}} + \frac{(\overline{p}_2 - \overline{p}_2^*)^2}{G_{p_2}},$$

with $\bar{t}_1^*$, $\bar{t}_2^*$, $\overline{p}_1^*$ and $\overline{p}_2^*$ defined by (A36).

By definition,

$$\begin{aligned}\Delta\mathcal{A} =& \frac{2\Delta\bar{t}_1(\bar{t}_1 - \bar{t}_1^*) + \left(\Delta\bar{t}_1\right)^2}{G_{t_1}} + \frac{2\Delta\bar{t}_2(\bar{t}_2 - \bar{t}_2^*) + \left(\Delta\bar{t}_2\right)^2}{G_{t_2}} \\ &+ \frac{2\Delta\overline{p}_1(\overline{p}_1 - \overline{p}_1^*) + (\Delta\overline{p}_1)^2}{G_{p_1}} + \frac{2\Delta\overline{p}_2(\overline{p}_2 - \overline{p}_2^*) + (\Delta\overline{p}_2)^2}{G_{p_2}}.\end{aligned}$$

When $\bar{t}_1 - \overline{p}_1$ and $\bar{t}_2 - \overline{p}_2$ are of order ε, $\Delta\bar{t}_1$, $\Delta\bar{t}_2$, $\Delta\overline{p}_1$ and $\Delta\overline{p}_2$ are of order ε^2. We then neglect the terms proportional to $\left(\Delta\bar{t}_1\right)^2$, $\left(\Delta\bar{t}_2\right)^2$, $(\Delta\overline{p}_1)^2$ or $(\Delta\overline{p}_2)^2$:

$$\Delta\mathcal{A} = \frac{2\Delta\bar{t}_1(\bar{t}_1 - \bar{t}_1^*)}{G_{t_1}} + \frac{2\Delta\bar{t}_2(\bar{t}_2 - \bar{t}_2^*)}{G_{t_2}} + \frac{2\Delta\overline{p}_1(\overline{p}_1 - \overline{p}_1^*)}{G_{p_1}} + \frac{2\Delta\overline{p}_2(\overline{p}_2 - \overline{p}_2^*)}{G_{p_2}} + O(\varepsilon^4).$$

By replacing the terms $\Delta\bar{t}_1$, $\Delta\bar{t}_2$, $\Delta\overline{p}_1$ and $\Delta\overline{p}_2$ using (12) and simplifying, we obtain:

$$\Delta\mathcal{A} = \beta_{t_1}(\overline{t_1} - \overline{t_1}^*) + \beta_{p_1}(\overline{p_1} - \overline{p_1}^*) + \beta_{t_2}(\overline{t_2} - \overline{t_2}^*) + \beta_{p_2}(\overline{p_2} - \overline{p_2}^*) + O(\varepsilon^4).$$

Using that for $i \in \{1, 2\}$, $\bar{t}_i - \overline{p}_i$ and $\bar{t}_i^* - \overline{p}_i^*$ are of order ε, we obtain similarly as in (A20)

$$\Delta\mathcal{A} = (\beta_{t_1} + \beta_{p_1})\left(\frac{\bar{t}_1 - \bar{t}_1^*}{2} + \frac{\overline{p}_1 - \overline{p}_1^*}{2}\right) + (\beta_{t_2} + \beta_{p_2})\left(\frac{\bar{t}_2 - \bar{t}_2^*}{2} + \frac{\overline{p}_2 - \overline{p}_2^*}{2}\right) + O(\varepsilon^3). \quad \text{(A37)}$$

Using (A26) and (A28) and simplifying, we obtain:

$$\beta_{t_1} + \beta_{p_1} = -\frac{4bd(\bar{t}_1 - \bar{t}_2)\lambda_2 N_2}{(1+\lambda_1 N_1 + \lambda_2 N_2)^2} - 4s_1(\bar{t}_1 - t_{a1}) + 2c_{RI}a_1(\bar{t}_1 - \bar{t}_2)\frac{N_2}{N_1} + O(\varepsilon^3).$$

By substracting $-\frac{4bd(\bar{t}_1^* - \bar{t}_2^*)\lambda_2 N_2}{(1+\lambda_1 N_1+\lambda_2 N_2)^2} - 4s_1(\bar{t}_1^* - t_{a1}) + 2c_{RI}a_1(\bar{t}_1^* - \bar{t}_2^*)\frac{N_2}{N_1}$ which is equal to zero (because $\beta_{t_1}|_{(t_1,t_2,p_1,p_2)=(\bar{t}_1^*,\bar{t}_2^*,\bar{p}_1^*,\bar{p}_2^*)} = 0$ and $\beta_{p_1}|_{(t_1,t_2,p_1,p_2)=(\bar{t}_1^*,\bar{t}_2^*,\bar{p}_1^*,\bar{p}_2^*)} = 0$, we get:

$$\begin{aligned}(\beta_{t_1} + \beta_{p_1}) &= \left(-\frac{4bd\lambda_2 N_2}{(1+\lambda_1 N_1 + \lambda_2 N_2)^2} - 4s_1 + 2c_{RI}a_1\frac{N_2}{N_1}\right)(\bar{t}_1 - \bar{t}_1^*) \\ &\quad - \left(-\frac{4bd\lambda_2 N_2}{(1+\lambda_1 N_1 + \lambda_2 N_2)^2} + 2c_{RI}a_1\frac{N_2}{N_1}\right)(\bar{t}_2 - \bar{t}_2^*) + O(\varepsilon^3) \\ &= -C_1(\bar{t}_1 - \bar{t}_1^*) + A_1C_1(\bar{t}_2 - \bar{t}_2^*) + O(\varepsilon^3).\end{aligned}$$

Because for $i \in \{1,2\}, \bar{t}_i - \bar{t}_i^* = \bar{p}_i - \bar{p}_i^* + \bar{t}_i - \bar{p}_i + \bar{p}_i^* - \bar{t}_i^* = \bar{p}_i - \bar{p}_i^* + O(\varepsilon)$ we also have

$$(\beta_{t_1} + \beta_{p_1}) = -C_1(\bar{p}_1 - \bar{p}_1^*) + A_1C_1(\bar{p}_2 - \bar{p}_2^*) + O(\varepsilon^3).$$

We thus get

$$(\beta_{t_1} + \beta_{p_1})(\bar{t}_1 - \bar{t}_1^*) = -C_1(\bar{t}_1 - \bar{t}_1^*)^2 + A_1C_1(\bar{t}_1 - \bar{t}_1^*)(\bar{t}_2 - \bar{t}_2^*) + O(\varepsilon^3),$$

and

$$(\beta_{t_1} + \beta_{p_1})(\bar{p}_1 - \bar{p}_1^*) = -C_1(\bar{p}_1 - \bar{p}_1^*)^2 + A_1C_1(\bar{p}_1 - \bar{p}_1^*)(\bar{p}_2 - \bar{p}_2^*) + O(\varepsilon^3).$$

Hence using (A37), the symmetry of the model between populations 1 and 2, and that for $i \in \{1,2\}$, $\bar{t}_i - \bar{p}_i$ and $\bar{t}_i^* - \bar{p}_i^*$ are of order ε, we obtain:

$$\begin{aligned}2\Delta\mathcal{A} = &-C_1(\bar{t}_1 - \bar{t}_1^*)^2 + (A_1C_1 + A_2C_2)(\bar{t}_1 - \bar{t}_1^*)(\bar{t}_2 - \bar{t}_2^*) - C_2(\bar{t}_2 - \bar{t}_2^*)^2 \\ &- C_1(\bar{p}_1 - \bar{p}_1^*)^2 + (A_1C_1 + A_2C_2)(\bar{p}_1 - \bar{p}_1^*)(\bar{p}_2 - \bar{p}_2^*) - C_2(\bar{p}_2 - \bar{p}_2^*)^2,\end{aligned}$$

with can be rewritten in matrix form

$$2\Delta\mathcal{A} = -T^tMT - P^tMP + O(\varepsilon^3),$$

with

$$M = \begin{pmatrix} C_1 & -\frac{A_1C_1+A_2C_2}{2} \\ -\frac{A_1C_1+A_2C_2}{2} & C_2 \end{pmatrix}, \quad T = \begin{pmatrix} \bar{t}_1 - \bar{t}_1^* \\ \bar{t}_2 - \bar{t}_2^* \end{pmatrix}, \quad P = \begin{pmatrix} \overline{p}_1 - \overline{p}_1^* \\ \overline{p}_2 - \overline{p}_2^* \end{pmatrix},$$

and T^t and P^t being the transposed of T and P respectively.

First case: $C_1 > 0$**,** $C_2 > 0$ **and** $C_1C_2(1 - A_1A_2) - \frac{1}{4}(A_1C_1 - A_2C_2)^2 > 0$**.**

According to the Sylvester's criterion the matrix M is positive-definite. Using computations similar to the ones derived to prove (A15), we may prove that after a number of generations large enough, $\bar{t}_1 - \bar{t}_1^*$, $\bar{t}_2 - \bar{t}_2^*$, $\overline{p}_1 - \overline{p}_1^*$ and $\overline{p}_2 - \overline{p}_2^*$ become of order $\varepsilon^{1/2}$.

Second case: $C_1 < 0$**,** $C_2 < 0$ **and** $C_1C_2(1 - A_1A_2) - \frac{1}{4}(A_1C_1 - A_2C_2)^2 > 0$**.**

According to the Sylvester's criterion the matrix $-M$ is positive-definite. Therefore $\bar{t}_1$, $\bar{t}_2$, $\overline{p}_1$ and $\overline{p}_2$ become very large.

□

2.5 Effect of different parameters on the level of trait divergence $|\bar{t}_1^* - \bar{t}_2^*|$ assuming weak or strong female choosiness and predator discrimination

We want to verify that the different parameters have similar effect on phenotypic distance between species in this model than in the first. To this aim we plot the effect of different parameters on the level of trait divergence assuming whether (H_w) (using the analytical approximation when possible or numerical simulations) or (H_s) (using numerical simulations). The following plots confirm that the parameters have a similar effect on the phenotypic distance.

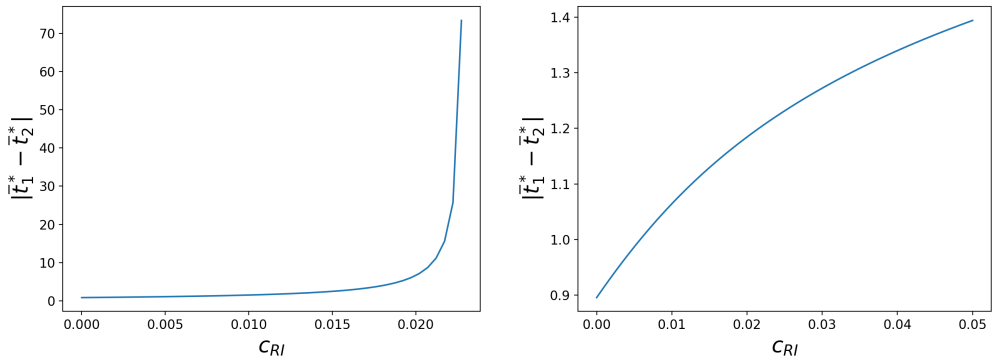

(a) (b)

Figure 11: **Influence of the strength of reproductive interference c_{RI} on the phenotypic distances between the focal species and the local mimicry rings, assuming (a) weak or (b) strong female choosiness and predator discrimination.** Simulations were run assuming (a) $a_1 = a_2 = b = 0.01$ or (b) $a_1 = a_2 = b = 1$. The default parameters values are as follows: $d = 0.02$, $\lambda_1 = 0.1$, $\lambda_2 = 0.1$, $N_1 = 10$, $N_2 = 20$, $s_1 = 0.0000025$, $s_2 = 0.0000025$, $t_{a1} = 0$, $t_{a2} = 1$.

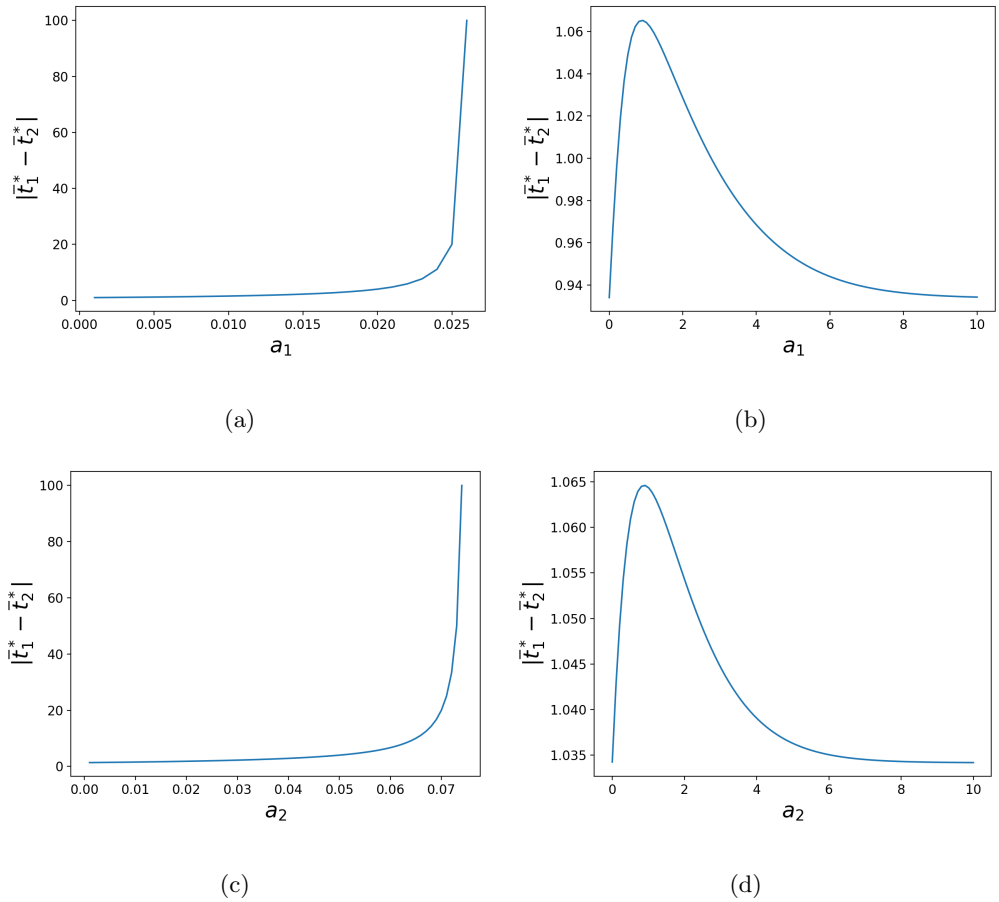

Figure 12: **Influence of female choosiness in species (a)(b) 1 a_1 and (c)(d) 2 a_1 on the phenotypic distances between the focal species and the local mimicry rings, assuming (a)(c) weak or (b)(d) strong female choosiness and predator discrimination.** Simulations were run assuming (a) $a_2 = b = 0.01$, (b) $a_2 = b = 1$, (c) $a_1 = b = 0.01$ or (d) $a_1 = b = 1$. The default parameters values are as follows: $c_{RI} = 0.01$, $d = 0.02$, $\lambda_1 = 0.1$, $\lambda_2 = 0.1$, $N_1 = 10$, $N_2 = 20$, $s_1 = 0.0000025$, $s_2 = 0.0000025$, $t_{a1} = 0$, $t_{a2} = 1$.

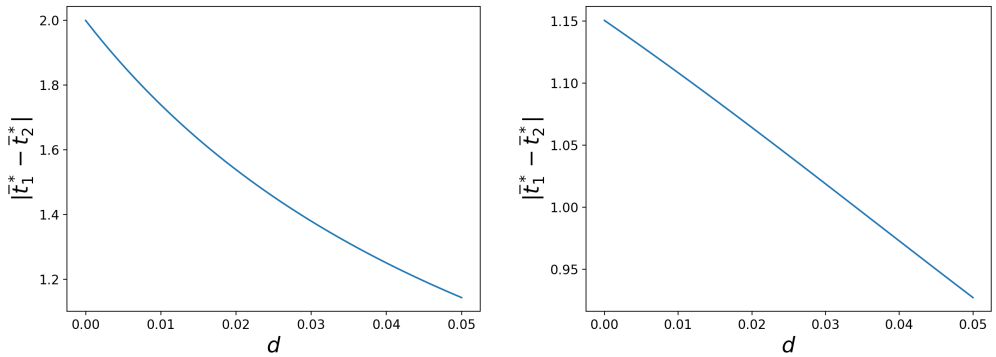

(a) (b)

Figure 13: **Influence of the strength of predation d on the phenotypic distances between the focal species and the local mimicry rings, assuming (a) weak or (b) strong female choosiness and predator discrimination.** Simulations were run assuming (a) $a_1 = a_2 = b = 0.01$, (b) $a_1 = a_2 = b = 1$. The default parameters values are as follows: $c_{RI} = 0.01$, $\lambda_1 = 0.1$, $\lambda_2 = 0.1$, $N_1 = 10$, $N_2 = 20$, $s_1 = 0.0000025$, $s_2 = 0.0000025$, $t_{a1} = 0$, $t_{a2} = 1$.

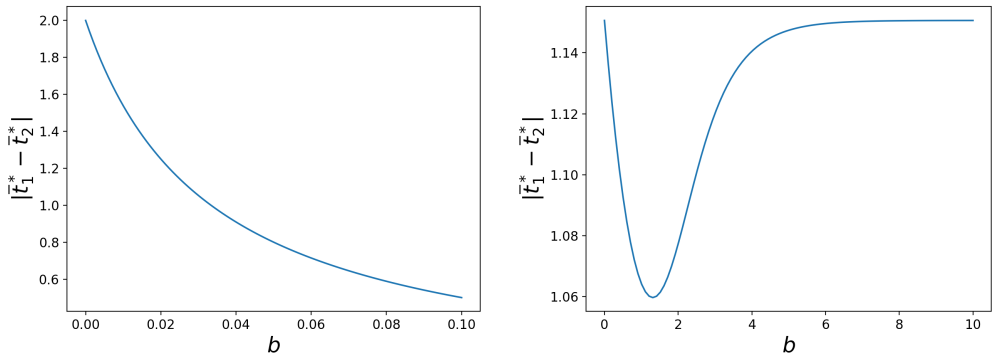

(a) (b)

Figure 14: **Influence of predator discrimination b on the phenotypic distances between the focal species and the local mimicry rings, assuming (a) weak or (b) strong female choosiness and predator discrimination.** Simulations were run assuming (a) $a_1 = a_2 = 0.01$, (b) $a_1 = a_2 = 1$. The default parameters values are as follows: $c_{RI} = 0.01$, $d = 0.02$, $\lambda_1 = 0.1$, $\lambda_2 = 0.1$, $N_1 = 10$, $N_2 = 20$, $s_1 = 0.0000025$, $s_2 = 0.0000025$, $t_{a1} = 0$, $t_{a2} = 1$.

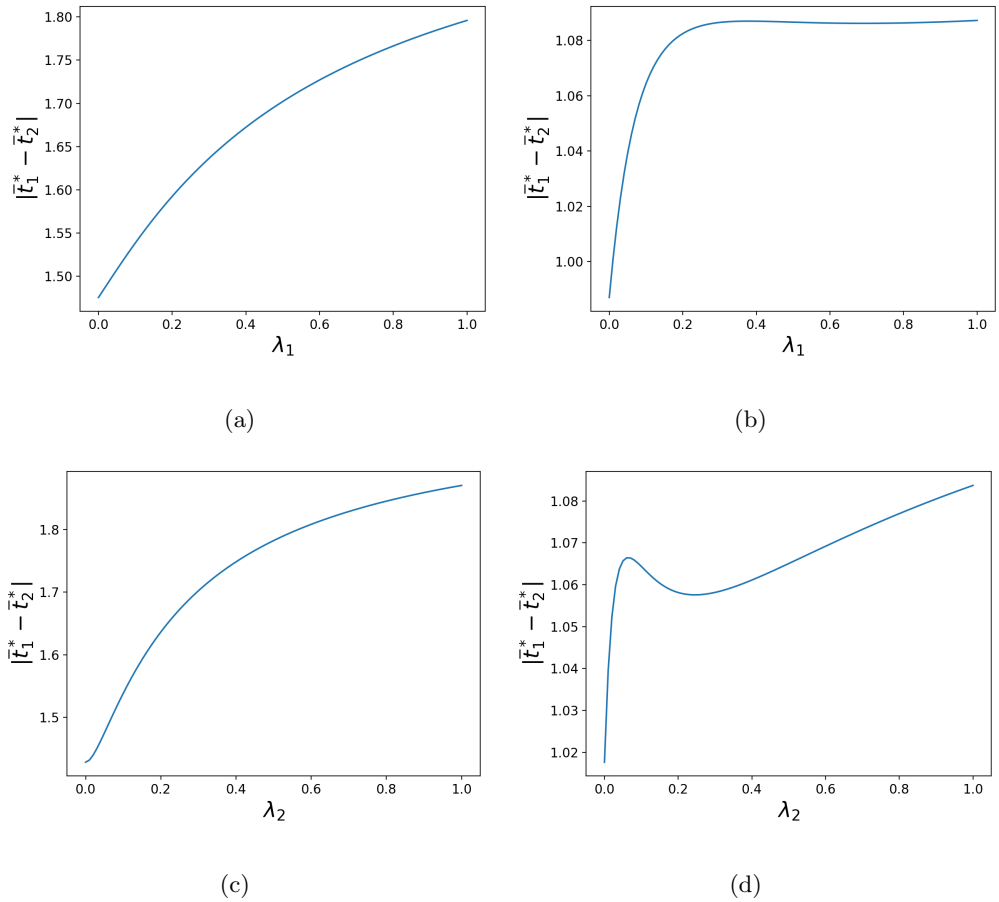

Figure 15: **Influence of the defence level of (a)(b) species 1 λ_1 and of (c)(d) species 2 λ_2 on the phenotypic distances between both species, assuming (a)(c) weak or (b)(d) strong female choosiness and predator discrimination.** Simulations were run assuming (a)(c) $a_1 = a_2 = b = 0.01$, (b)(d) $a_1 = a_2 = b = 1$. The default parameters values are as follows: $c_{RI} = 0.01$, $d = 0.02$, $\lambda_1 = 0.1$, $\lambda_2 = 0.1$, $N_1 = 10$, $N_2 = 20$, $s_1 = 0.0000025$, $s_2 = 0.0000025$, $t_{a1} = 0$, $t_{a2} = 1$.

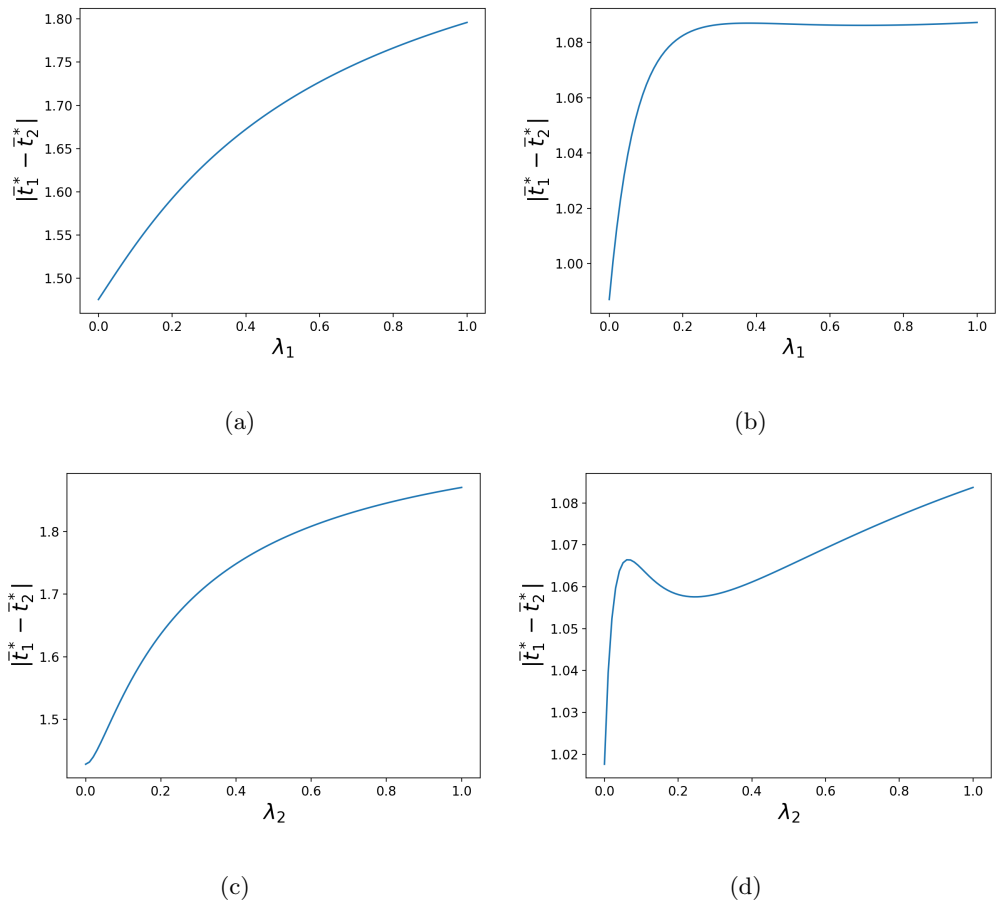

Figure 16: **Influence of the defence level of (a)(b) species 1 λ_1 and of (c)(d) species 2 λ_2 on the phenotypic distances between both species, assuming (a)(c) weak or (b)(d) strong female choosiness and predator discrimination.** Simulations were run assuming (a)(c) $a_1 = a_2 = b = 0.01$, (b)(d) $a_1 = a_2 = b = 1$. The default parameters values are as follows: $c_{RI} = 0.01$, $d = 0.02$, $\lambda_1 = 0.1$, $\lambda_2 = 0.1$, $N_1 = 10$, $N_2 = 20$, $s_1 = 0.0000025$, $s_2 = 0.0000025$, $t_{a1} = 0$, $t_{a2} = 1$.

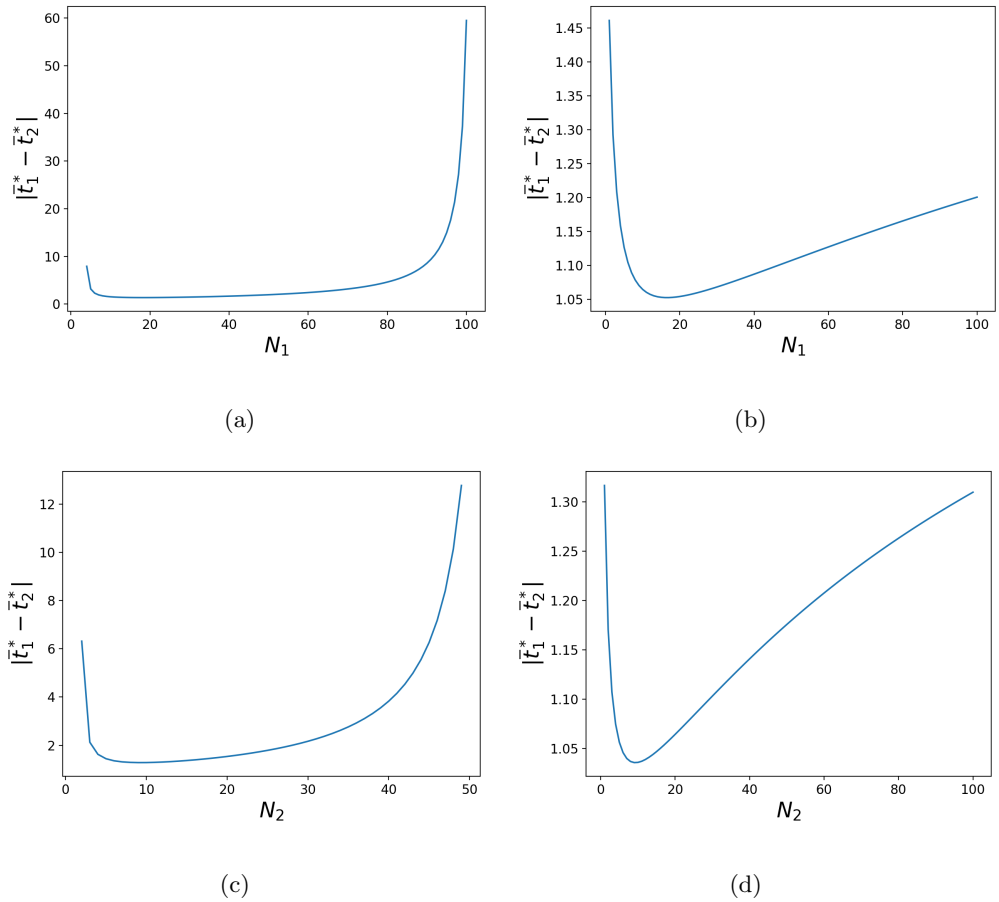

Figure 17: **Influence of the density of (a)(b) species 1 N_1 and of (c)(d) species 2 N_2 on the phenotypic distances between the focal species and the local mimicry rings, assuming (a)(c) weak or (b)(d) strong female choosiness and predator discrimination.** Simulations were run assuming (a) $a_1 = a_2 = b = 0.01$, (b) $a_1 = a_2 = b = 1$. The default parameters values are as follows: $c_{RI} = 0.01$, $d = 0.02$, $\lambda_1 = 0.1$, $\lambda_2 = 0.1$, $N_1 = 10$, $N_2 = 20$, $s_1 = 0.0000025$, $s_2 = 0.0000025$, $t_{a1} = 0$, $t_{a2} = 1$.

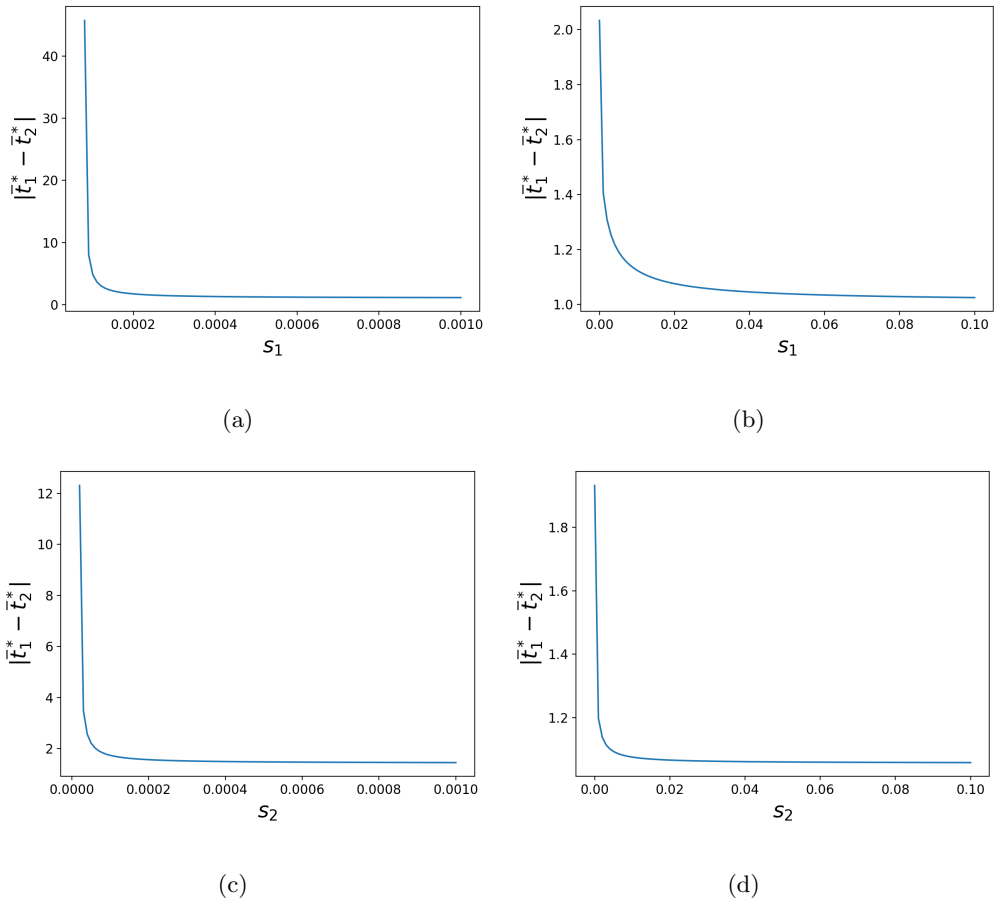

Figure 18: **Influence of the strength of selective constraints in (a)(b) species 1 s_1 and in (c)(d) species 2 s_2 on the phenotypic distances between the focal species and the local mimicry rings, assuming (a)(c) weak or (b)(d) strong female choosiness and predator discrimination.** Simulations were run assuming (a)(c) $a_1 = a_2 = b = 0.01$, (b)(d) $a_1 = a_2 = b = 1$. The default parameters values are as follows: $c_{RI} = 0.01$, $d = 0.02$, $\lambda_1 = 0.1$, $\lambda_2 = 0.1$, $N_1 = 10$, $N_2 = 20$, $s_1 = 0.0000025$, $s_2 = 0.0000025$, $t_{a1} = 0$, $t_{a2} = 1$.

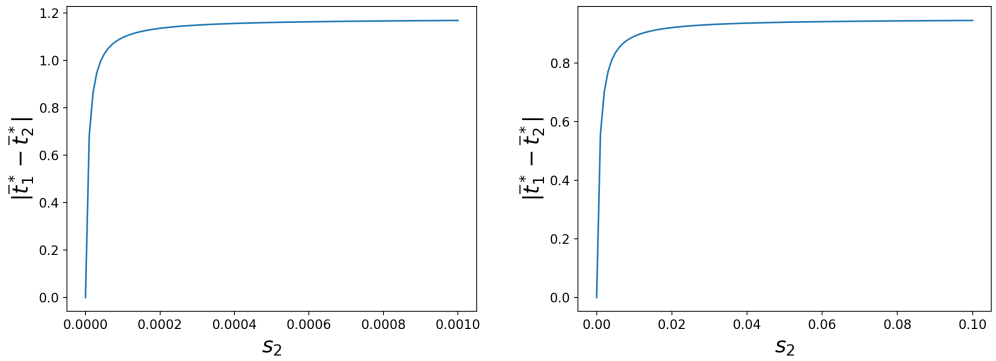

(a) (b)

Figure 19: **Influence of the strength of selective constraints in species 2 s_2 on the phenotypic distances between the focal species and the local mimicry rings, when predation is great compare to RI, assuming (a) weak or (b) strong female choosiness and predator discrimination.** Simulations were run assuming (a) $a_1 = a_2 = b = 0.01$, (b) $a_1 = a_2 = b = 1$. The default parameters values are as follows: $c_{RI} = 0.01$, $d = 0.05$, $\lambda_1 = 0.1$, $\lambda_2 = 0.1$, $N_1 = 10$, $N_2 = 20$, $s_1 = 0.0000025$, $s_2 = 0.0000025$, $t_{a1} = 0$, $t_{a2} = 1$.

References

N. H. Barton and M. Turelli. Natural and sexual selection on many loci. Genetics, 127 (1):229–255, 1991. ISSN 0016-6731. URL https://www.genetics.org/content/127/1/229.

M. Kirkpatrick, T. Johnson, and N. Barton. General models of multilocus evolution. Genetics, 161(4):1727–1750, 2002. ISSN 0016-6731. URL https://www.genetics.org/content/161/4/1727.

R. Lande. Models of speciation by sexual selection on polygenic traits. Proceedings of the National Academy of Sciences, 78(6):3721–3725, 1981. ISSN 0027-8424. 10.1073/pnas.78.6.3721. URL https://www.pnas.org/content/78/6/3721.

A. Pomiankowski and Y. Iwasa. Evolution of multiple sexual preferences by fisher's runaway process of sexual selection. Proceedings: Biological Sciences, 253(1337):173–181, 1993. ISSN 09628452. URL http://www.jstor.org/stable/49806.